Electronic Supplementary Material (ESI) for Physical Chemistry Chemical Physics.

Electronic Supplementary Information

Infrared spectra of isoquinolinium (*iso*-$C_9H_7NH^+$) and isoquinolinyl radicals (*iso*-C_9H_7NH and 1-, 3-, 4-, 5-, 6-, 7-, and 8-*iso*-HC_9H_7N) isolated in solid *para*-Hydrogen

Prasad Ramesh Joshi,*[a] Masashi Tsuge,*[b] Chih-Yu Tseng,[a] and Yuan-Pern Lee*[ac]

[a] Department of Applied Chemistry and Institute of Molecular Science, National Yang Ming Chiao Tung University, Hsinchu 300093, Taiwan
[b] Institute of Low Temperature Science, Hokkaido University, Sapporo 060-0819, Japan
[c] Center for Emergent Functional Matter Science, National Yang Ming Chiao Tung University, Hsinchu 300093, Taiwan

E-mail: prasad.nctu@gmail.com, tsuge@lowtem.hokudai.ac.jp and yplee@nctu.edu.tw

Table of Contents

Table S1 Comparison of observed vibrational wavenumbers (in cm^{-1}) and relative IR intensities of lines in group A$^+$ with scaled harmonic and anharmonic vibrational wavenumbers and IR intensities of *iso*-$C_9H_7NH^+$ predicted with the B3LYP/6-311++G(d,p) method

Mode	Sym.	Calculations		Experiments	
		Scaled harmonic	Anharmonic	IRMPD[a]	*p*-H_2
ν_1	a'	3430[b] (208)[c]	3407 (180)[c]		3397.2 (250)[d]
ν_2	a'	3128 (8)	3119 (2)		
ν_3	a'	3104 (5)	3072 (0)		
ν_4	a'	3100 (0)	3079 (2)		
ν_5	a'	3099 (2)	3057 (4)		
ν_6	a'	3092 (0)	3078 (0)		
ν_7	a'	3083 (0)	3065 (1)		
ν_8	a'	3079 (0)	3030 (1)		
ν_9	a'	1639 (83)	1625 (60)	1582	1643.3 (40)
ν_{10}	a'	1620 (27)	1610 (19)		
ν_{11}	a'	1587 (15)	1576 (11)		
ν_{12}	a'	1559 (7)	1550 (10)		1554.7 (10)
ν_{13}	a'	1500 (14)	1494 (12)		1497.3 (7)
ν_{14}	a'	1469 (6)	1466 (4)		
ν_{15}	a'	1420 (3)	1418 (2)		
ν_{16}	a'	1394 (43)	1382 (40)	1360	1400.1 (69)
ν_{17}	a'	1382 (49)	1378 (25)		1378.6 (31)
ν_{18}	a'	1285 (13)	1285 (12)		
ν_{19}	a'	1274 (9)	1274 (6)		
ν_{20}	a'	1263 (1)	1261 (3)		
ν_{21}	a'	1221 (3)	1222 (1)		
ν_{22}	a'	1177 (5)	1183 (3)		
ν_{23}	a'	1174 (4)	1176 (4)		
ν_{24}	a'	1150 (3)	1153 (2)		
ν_{25}	a'	1032 (9)	1031 (7)		
ν_{26}	a'	1019 (4)	1018 (5)		
ν_{27}	a'	951 (2)	952 (1)		
ν_{28}	a'	803 (1)	806 (1)		
ν_{29}	a'	764 (1)	763 (0)		
ν_{30}	a'	634 (2)	637 (2)		
ν_{31}	a'	514 (0)	517 (0)		
ν_{32}	a'	504 (1)	507 (1)		
ν_{33}	a'	360 (3)	364 (3)		
ν_{34}	a"	1018 (0)	1004 (0)		
ν_{35}	a"	987 (2)	988 (2)		
ν_{36}	a"	962 (2)	975 (0)		
ν_{37}	a"	935 (2)	948 (2)		
ν_{38}	a"	882 (2)	891 (2)		
ν_{39}	a"	829 (6)	834 (5)		
ν_{40}	a"	788 (150)	806 (39)	774	791.4 (100)
ν_{41}	a"	750 (3)	762 (56)		
ν_{42}	a"	724 (23)	715 (58)		
ν_{43}	a"	613 (1)	612 (0)		
ν_{44}	a"	471 (29)	471 (32)		
ν_{45}	a"	455 (1)	440 (0)		
ν_{46}	a"	386 (0)	382 (0)		
ν_{47}	a"	178 (0)	177 (0)		
ν_{48}	a"	166 (8)	165 (8)		

[a] Infrared multiphoton dissociation (IRMPD) experiments by Galué *et al.* (*Astron. Astrophys.* **2010,** *517*, A15). [b] Harmonic vibrational wavenumbers scaled according to $0.9122\, x + 174.3$ for wavenumbers >2000 cm^{-1} and $0.9823\, x + 0.6$ for wavenumbers <2000 cm^{-1}. [c] IR intensities in km mol^{-1} are listed in parentheses. [d] IR intensities as per cent of that of the line at 791.4 cm^{-1} are listed in parentheses.

Table S2 Scaled harmonic and anharmonic vibrational wavenumbers and IR intensities of 1-, 3-, and 4-*iso*-$H^+C_9H_7N$ cations calculated with the B3LYP/6-311++G(d,p) method

Mode	1-*iso*-$H^+C_9H_7N$		3-*iso*-$H^+C_9H_7N$		4-*iso*-$H^+C_9H_7N$	
	Scaled harm.^{a}	Anharmonic	Scaled harm.^{a}	Anharmonic	Scaled harm.^{a}	Anharmonic
ν_1	3102 (1)^b	3118 (0)^b	3102 (1)^b	3109 (0)^b	3102 (1)^b	3099 (0)^b
ν_2	3088 (1)	3091 (0)	3090 (1)	3083 (0)	3089 (0)	3083 (0)
ν_3	3085 (0)	3060 (0)	3084 (0)	3068 (0)	3083 (0)	3064 (0)
ν_4	3077 (0)	3038 (0)	3080 (0)	3030 (1)	3077 (0)	3045 (2)
ν_5	3072 (0)	3052 (1)	3060 (1)	3017 (2)	3058 (3)	3037 (1)
ν_6	3058 (2)	3025 (1)	3038 (2)	3023 (1)	3046 (1)	3025 (1)
ν_7	2884 (54)	2827 (48)	2866 (91)	2808 (82)	2890 (31)	2837 (24)
ν_8	1631 (72)	1619 (55)	1620 (38)	1606 (28)	1623 (149)	1612 (57)
ν_9	1583 (68)	1572 (28)	1606 (168)	1598 (121)	1570 (68)	1563 (42)
ν_{10}	1538 (11)	1530 (11)	1549 (4)	1539 (7)	1551 (3)	1541 (9)
ν_{11}	1501 (154)	1491 (111)	1518 (59)	1509 (6)	1500 (186)	1490 (116)
ν_{12}	1468 (38)	1457 (27)	1474 (37)	1465 (21)	1452 (134)	1446 (42)
ν_{13}	1429 (15)	1428 (3)	1430 (15)	1424 (13)	1435 (149)	1423 (90)
ν_{14}	1399 (34)	1396 (51)	1394 (47)	1390 (56)	1390 (60)	1387 (35)
ν_{15}	1382 (55)	1369 (34)	1377 (33)	1366 (8)	1376 (49)	1368 (27)
ν_{16}	1327 (17)	1317 (5)	1314 (13)	1298 (9)	1348 (19)	1333 (12)
ν_{17}	1297 (109)	1274 (72)	1280 (35)	1282 (19)	1317 (141)	1297 (123)
ν_{18}	1270 (20)	1262 (10)	1273 (202)	1252 (192)	1284 (59)	1282 (24)
ν_{19}	1241 (14)	1233 (7)	1245 (8)	1245 (12)	1257 (14)	1257 (1)
ν_{20}	1196 (19)	1196 (11)	1210 (21)	1210 (18)	1195 (13)	1197 (8)
ν_{21}	1175 (15)	1179 (19)	1182 (6)	1190 (5)	1177 (9)	1181 (10)
ν_{22}	1132 (6)	1133 (5)	1135 (6)	1136 (7)	1154 (65)	1156 (17)
ν_{23}	1073 (2)	1074 (3)	1057 (13)	1052 (12)	1133 (6)	1134 (5)
ν_{24}	1021 (6)	1022 (3)	1021 (4)	1024 (4)	1026 (2)	1028 (1)
ν_{25}	962 (39)	963 (35)	936 (8)	936 (5)	955 (4)	955 (4)
ν_{26}	918 (16)	922 (14)	898 (50)	899 (49)	909 (4)	912 (5)
ν_{27}	789 (6)	792 (6)	772 (1)	777 (1)	788 (9)	783 (6)
ν_{28}	741 (9)	743 (8)	749 (5)	752 (4)	748 (3)	747 (3)
ν_{29}	609 (0)	614 (0)	622 (1)	627 (1)	620 (5)	624 (4)
ν_{30}	509 (17)	508 (8)	514 (4)	515 (4)	506 (1)	512 (0)
ν_{31}	478 (9)	481 (9)	484 (8)	487 (8)	489 (3)	484 (1)
ν_{32}	346 (0)	349 (0)	350 (1)	354 (1)	348 (0)	354 (0)
ν_{33}	2885 (14)	2812 (13)	2858 (16)	2785 (15)	2898 (11)	2828 (10)
ν_{34}	1188 (2)	1170 (1)	1176 (0)	1159 (0)	1166 (0)	1156 (0)
ν_{35}	1022 (1)	1027 (0)	1025 (2)	1037 (0)	1022 (0)	1019 (0)
ν_{36}	1021 (1)	1016 (0)	1002 (8)	1010 (5)	1005 (4)	1031 (2)
ν_{37}	990 (1)	988 (1)	976 (8)	978 (3)	978 (0)	983 (0)
ν_{38}	935 (3)	947 (1)	954 (2)	964 (7)	967 (0)	977 (0)
ν_{39}	875 (19)	870 (13)	881 (1)	887 (1)	877 (1)	877 (0)
ν_{40}	839 (4)	837 (1)	789 (27)	779 (36)	772 (50)	808 (3)
ν_{41}	774 (36)	776 (28)	769 (22)	809 (0)	753 (20)	753 (51)
ν_{42}	670 (14)	692 (15)	689 (5)	696 (9)	643 (0)	664 (0)
ν_{43}	468 (1)	473 (2)	475 (22)	480 (17)	441 (15)	443 (14)
ν_{44}	426 (1)	432 (1)	434 (7)	442 (10)	407 (0)	421 (3)
ν_{45}	401 (8)	399 (9)	391 (12)	393 (12)	376 (3)	396 (2)
ν_{46}	251 (25)	257 (25)	271 (2)	280 (2)	211 (10)	224 (10)
ν_{47}	167 (1)	166 (1)	165 (1)	165 (1)	133 (0)	146 (1)
ν_{48}	111 (1)	115 (0)	127 (5)	131 (5)	109 (4)	118 (3)

^{a} Harmonic vibrational wavenumbers scaled according to 0.9122 x + 174.3 for wavenumbers >2000 cm^{-1} and 0.9823 x + 0.6 for wavenumbers <2000 cm^{-1}. ^{b} IR intensities in km mol^{-1} are listed in parentheses.

Table S3 Scaled harmonic and anharmonic vibrational wavenumbers and IR intensities of 5-, 6-, and 7-*iso*-$H^+C_9H_7N$ cations calculated with the B3LYP/6-311++G(d,p) method

Mode	5-*iso*-$H^+C_9H_7N$		6-*iso*-$H^+C_9H_7N$		7-*iso*-$H^+C_9H_7N$	
	Scaled harm.[a]	Anharmonic	Scaled harm.[a]	Anharmonic	Scaled harm.[a]	Anharmonic
ν_1	3101 (3)	3090 (1)	3096 (0)	3085 (1)	3094 (0)	3092 (0)
ν_2	3087 (0)	3072 (1)	3095 (2)	3076 (1)	3093 (1)	3061 (0)
ν_3	3077 (3)	3060 (6)	3084 (3)	3068 (4)	3081 (2)	3076 (0)
ν_4	3073 (2)	3044 (0)	3081 (2)	3086 (1)	3077 (2)	3032 (2)
ν_5	3066 (0)	3029 (1)	3071 (3)	3051 (1)	3066 (2)	3024 (1)
ν_6	3050 (1)	3019 (0)	3058 (2)	3037 (2)	3046 (1)	3026 (1)
ν_7	2860 (32)	2840 (23)	2865 (77)	2807 (63)	2874 (62)	2820 (38)
ν_8	1617 (154)	1605 (120)	1617 (108)	1609 (45)	1636 (370)	1623 (292)
ν_9	1573 (205)	1563 (93)	1579 (34)	1569 (30)	1594 (104)	1584 (111)
ν_{10}	1545 (65)	1532 (79)	1523 (8)	1515 (4)	1538 (2)	1529 (4)
ν_{11}	1509 (104)	1504 (38)	1471 (78)	1461 (29)	1497 (16)	1487 (22)
ν_{12}	1461 (174)	1453 (58)	1449 (21)	1438 (13)	1478 (115)	1465 (78)
ν_{13}	1427 (7)	1423 (8)	1439 (9)	1434 (13)	1427 (1)	1423 (2)
ν_{14}	1394 (61)	1387 (47)	1394 (2)	1391 (6)	1377 (15)	1374 (141)
ν_{15}	1363 (1)	1351 (1)	1358 (7)	1331 (59)	1375 (48)	1365 (54)
ν_{16}	1333 (23)	1322 (19)	1337 (116)	1316 (34)	1353 (60)	1331 (19)
ν_{17}	1321 (121)	1297 (88)	1281 (69)	1283 (24)	1299 (126)	1287 (51)
ν_{18}	1266 (26)	1262 (18)	1264 (170)	1246 (102)	1275 (65)	1268 (89)
ν_{19}	1254 (36)	1252 (6)	1248 (37)	1243 (32)	1252 (7)	1252 (7)
ν_{20}	1215 (40)	1212 (34)	1209 (8)	1208 (10)	1231 (37)	1227 (37)
ν_{21}	1184 (16)	1188 (10)	1183 (16)	1184 (12)	1184 (24)	1185 (18)
ν_{22}	1160 (20)	1157 (15)	1153 (42)	1155 (42)	1163 (28)	1166 (22)
ν_{23}	1096 (24)	1099 (22)	1050 (4)	1054 (5)	1046 (26)	1045 (18)
ν_{24}	1049 (3)	1052 (3)	1027 (18)	1024 (18)	1024 (3)	1023 (5)
ν_{25}	953 (6)	955 (6)	924 (2)	927 (4)	925 (8)	929 (7)
ν_{26}	913 (9)	911 (8)	914 (20)	913 (11)	907 (32)	909 (31)
ν_{27}	791 (1)	794 (1)	772 (12)	775 (12)	774 (1)	778 (0)
ν_{28}	751 (10)	752 (10)	753 (11)	756 (10)	751 (3)	752 (3)
ν_{29}	622 (2)	627 (2)	629 (4)	633 (4)	629 (2)	633 (2)
ν_{30}	504 (10)	507 (8)	505 (5)	508 (2)	510 (0)	514 (0)
ν_{31}	485 (0)	487 (0)	491 (6)	490 (6)	487 (1)	486 (0)
ν_{32}	348 (0)	351 (0)	352 (1)	357 (1)	352 (1)	356 (1)
ν_{33}	2896 (10)	2829 (9)	2859 (18)	2785 (18)	2871 (13)	2800 (12)
ν_{34}	1164 (1)	1152 (1)	1130 (0)	1112 (0)	1147 (0)	1132 (0)
ν_{35}	1025 (0)	1032 (0)	1006 (0)	1011 (0)	1009 (1)	1019 (0)
ν_{36}	1008 (5)	1005 (3)	988 (1)	1035 (1)	1005 (2)	1046 (2)
ν_{37}	1000 (0)	1017 (2)	944 (28)	948 (15)	956 (13)	982 (5)
ν_{38}	933 (2)	959 (2)	925 (0)	962 (8)	915 (10)	939 (17)
ν_{39}	874 (2)	876 (0)	813 (31)	841 (9)	860 (26)	871 (26)
ν_{40}	843 (22)	843 (17)	798 (2)	810 (8)	799 (6)	793 (0)
ν_{41}	731 (35)	749 (31)	765 (0)	785 (7)	781 (4)	821 (1)
ν_{42}	668 (0)	670 (1)	669 (21)	677 (17)	663 (1)	679 (3)
ν_{43}	494 (13)	504 (12)	471 (0)	486 (0)	496 (42)	502 (42)
ν_{44}	427 (13)	434 (16)	449 (20)	463 (25)	391 (0)	425 (0)
ν_{45}	340 (1)	344 (0)	348 (1)	358 (1)	337 (1)	359 (0)
ν_{46}	242 (7)	247 (7)	240 (10)	249 (9)	247 (1)	255 (1)
ν_{47}	172 (0)	171 (0)	160 (0)	164 (0)	166 (1)	169 (1)
ν_{48}	116 (0)	121 (0)	136 (1)	142 (1)	130 (4)	137 (4)

[a] Harmonic vibrational wavenumbers scaled according to 0.9122 x + 174.3 for wavenumbers >2000 cm^{-1} and 0.9823 x + 0.6 for wavenumbers <2000 cm^{-1}. [b] IR intensities in km mol^{-1} are listed in parentheses.

Table S4 Scaled harmonic and anharmonic vibrational wavenumbers and IR intensities of 8-, 4a-, and 8a-*iso*-H$^+$C$_9$H$_7$N cations calculated with the B3LYP/6-311++G(d,p) method

Mode	8-*iso*-H$^+$C$_9$H$_7$N		4a-*iso*-H$^+$C$_9$H$_7$N		8a-*iso*-H$^+$C$_9$H$_7$N	
	Scaled harm.[a]	Anharmonic	Scaled harm.[a]	Anharmonic	Scaled harm.[a]	Anharmonic
ν_1	3100 (4)	3096 (3)	3098 (4)	3082 (1)	3099 (2)	3073 (0)
ν_2	3093 (0)	3079 (1)	3097 (0)	3073 (0)	3094 (1)	3077 (0)
ν_3	3080 (2)	3068 (2)	3090 (3)	3068 (0)	3091 (2)	3064 (4)
ν_4	3076 (3)	3058 (0)	3084 (3)	3075 (3)	3082 (3)	3080 (1)
ν_5	3068 (0)	3033 (1)	3082 (0)	3063 (1)	3081 (1)	3113 (0)
ν_6	3052 (2)	3026 (1)	3079 (1)	3042 (0)	3078 (1)	3044 (0)
ν_7	2877 (44)	2820 (10)	3051 (1)	3027 (2)	3040 (1)	3023 (1)
ν_8	1601 (18)	1588 (14)	2635 (58)	2537 (50)	2692 (47)	2608 (37)
ν_9	1558 (58)	1551 (15)	1608 (26)	1597 (7)	1622 (139)	1609 (43)
ν_{10}	1543 (9)	1537 (1)	1586 (41)	1571 (7)	1609 (93)	1597 (73)
ν_{11}	1488 (211)	1478 (141)	1539 (3)	1530 (2)	1548 (19)	1536 (1)
ν_{12}	1459 (87)	1452 (74)	1495 (22)	1486 (8)	1493 (21)	1488 (10)
ν_{13}	1428 (7)	1427 (1)	1437 (33)	1434 (13)	1454 (38)	1450 (2)
ν_{14}	1414 (59)	1410 (6)	1418 (2)	1409 (2)	1421 (155)	1412 (2)
ν_{15}	1359 (3)	1346 (1)	1380 (49)	1378 (13)	1401 (43)	1391 (40)
ν_{16}	1308 (46)	1296 (36)	1374 (196)	1368 (99)	1388 (99)	1379 (70)
ν_{17}	1294 (133)	1273 (63)	1352 (21)	1336 (12)	1335 (0)	1326 (0)
ν_{18}	1268 (59)	1263 (41)	1255 (24)	1254 (11)	1257 (4)	1262 (1)
ν_{19}	1245 (33)	1240 (16)	1239 (21)	1235 (13)	1230 (37)	1228 (29)
ν_{20}	1194 (9)	1192 (12)	1187 (5)	1188 (10)	1208 (31)	1209 (15)
ν_{21}	1187 (8)	1191 (5)	1182 (13)	1186 (8)	1180 (20)	1187 (21)
ν_{22}	1159 (21)	1157 (20)	1162 (3)	1159 (1)	1144 (8)	1142 (6)
ν_{23}	1100 (2)	1103 (0)	1133 (5)	1136 (3)	1123 (7)	1110 (4)
ν_{24}	1057 (2)	1057 (2)	1028 (2)	1028 (1)	1030 (3)	1021 (2)
ν_{25}	953 (9)	956 (9)	1024 (4)	1023 (3)	1024 (5)	1031 (6)
ν_{26}	913 (9)	913 (9)	1009 (1)	1014 (0)	1017 (3)	1011 (1)
ν_{27}	786 (3)	787 (2)	1007 (1)	997 (0)	1013 (5)	1007 (1)
ν_{28}	759 (1)	759 (1)	1001 (1)	991 (1)	1000 (2)	996 (5)
ν_{29}	618 (7)	623 (6)	948 (9)	949 (7)	984 (17)	969 (10)
ν_{30}	505 (8)	507 (7)	914 (17)	915 (18)	948 (18)	929 (10)
ν_{31}	487 (14)	489 (14)	900 (15)	885 (3)	919 (14)	918 (6)
ν_{32}	346 (0)	350 (0)	880 (31)	847 (31)	900 (17)	892 (19)
ν_{33}	2879 (12)	2805 (11)	823 (51)	782 (20)	849 (37)	843 (30)
ν_{34}	1148 (1)	1135 (0)	803 (57)	805 (48)	831 (42)	822 (11)
ν_{35}	1028 (0)	1038 (0)	768 (7)	764 (21)	770 (6)	772 (9)
ν_{36}	1005 (4)	1017 (2)	719 (50)	714 (51)	732 (44)	731 (27)
ν_{37}	989 (1)	1001 (2)	713 (2)	716 (1)	719 (40)	720 (26)
ν_{38}	935 (0)	963 (1)	694 (34)	679 (53)	712 (1)	709 (25)
ν_{39}	863 (21)	867 (12)	622 (3)	624 (7)	620 (1)	624 (1)
ν_{40}	822 (22)	825 (26)	557 (20)	557 (20)	531 (10)	533 (9)
ν_{41}	722 (9)	752 (1)	507 (3)	509 (3)	502 (4)	505 (4)
ν_{42}	680 (17)	678 (19)	477 (18)	479 (16)	480 (1)	482 (0)
ν_{43}	490 (8)	496 (6)	448 (14)	447 (14)	462 (18)	462 (18)
ν_{44}	402 (6)	417 (9)	426 (2)	425 (2)	418 (2)	417 (1)
ν_{45}	387 (4)	392 (5)	335 (1)	338 (1)	335 (1)	337 (1)
ν_{46}	239 (6)	253 (7)	324 (1)	324 (1)	302 (3)	303 (2)
ν_{47}	165 (1)	167 (1)	156 (1)	156 (1)	144 (1)	145 (1)
ν_{48}	123 (4)	130 (3)	148 (1)	149 (1)	141 (2)	142 (2)

[a] Harmonic vibrational wavenumbers scaled according to $0.9122\,x + 174.3$ for wavenumbers >2000 cm^{-1} and $0.9823\,x + 0.6$ for wavenumbers <2000 cm^{-1}. [b] IR intensities in km mol^{-1} are listed in parentheses.

Table S5 Scaled harmonic and anharmonic vibrational wavenumbers and IR intensities of *iso*-C_9H_7NH, 1-, and 3-*iso*-HC_9H_7N radicals calculated with the B3LYP/6-311++G(d,p) method

Mode	*iso*-C_9H_7NH		1-*iso*-HC_9H_7N		3-*iso*-HC_9H_7N	
	Scaled harm.[a]	Anharmonic	Scaled harm.[a]	Anharmonic	Scaled harm.[a]	Anharmonic
ν_{1}	3518 (107)	3476 (58)	3083 (17)	3068 (4)	3085 (16)	3072 (22)
ν_{2}	3115 (5)	3094 (7)	3076 (21)	3052 (6)	3072 (21)	3047 (21)
ν_{3}	3101 (12)	3071 (9)	3070 (15)	3076 (34)	3059 (2)	3063 (9)
ν_{4}	3083 (15)	3074 (13)	3058 (1)	3020 (16)	3054 (20)	3004 (12)
ν_{5}	3082 (5)	3067 (81)	3049 (8)	3001 (6)	3054 (0)	3026 (5)
ν_{6}	3066 (27)	3051 (43)	3012 (37)	2988 (39)	2985 (35)	2922 (26)
ν_{7}	3053 (6)	3042 (10)	2884 (18)	2827 (10)	2864 (42)	2789 (23)
ν_{8}	3050 (10)	3006 (1)	1596 (1)	1583 (1)	1644 (57)	1623 (35)
ν_{9}	1614 (48)	1603 (31)	1567 (4)	1556 (2)	1573 (5)	1562 (3)
ν_{10}	1577 (20)	1565 (6)	1513 (9)	1502 (6)	1538 (11)	1530 (7)
ν_{11}	1541 (7)	1530 (2)	1482 (5)	1473 (3)	1477 (1)	1471 (1)
ν_{12}	1489 (11)	1484 (10)	1442 (2)	1435 (1)	1440 (2)	1435 (0)
ν_{13}	1478 (25)	1465 (2)	1414 (14)	1398 (11)	1422 (2)	1419 (2)
ν_{14}	1440 (17)	1436 (10)	1394 (5)	1386 (2)	1400 (4)	1385 (2)
ν_{15}	1411 (14)	1401 (7)	1348 (0)	1342 (0)	1374 (2)	1372 (0)
ν_{16}	1392 (5)	1389 (4)	1326 (2)	1316 (1)	1322 (2)	1324 (1)
ν_{17}	1316 (4)	1312 (2)	1281 (4)	1267 (5)	1307 (1)	1284 (1)
ν_{18}	1271 (4)	1273 (3)	1253 (1)	1248 (1)	1265 (5)	1264 (4)
ν_{19}	1231 (0)	1233 (2)	1217 (4)	1215 (2)	1227 (14)	1223 (7)
ν_{20}	1207 (4)	1212 (4)	1184 (6)	1179 (3)	1181 (8)	1182 (4)
ν_{21}	1181 (22)	1165 (14)	1158 (1)	1163 (2)	1145 (6)	1150 (4)
ν_{22}	1147 (5)	1145 (5)	1119 (2)	1118 (1)	1118 (5)	1123 (3)
ν_{23}	1129 (2)	1128 (3)	1069 (7)	1071 (7)	1034 (10)	1032 (9)
ν_{24}	1115 (10)	1115 (16)	1034 (1)	1033 (1)	1018 (5)	1017 (5)
ν_{25}	1026 (6)	1026 (5)	945 (10)	942 (3)	933 (1)	934 (1)
ν_{26}	982 (90)	980 (61)	920 (16)	920 (14)	870 (32)	871 (26)
ν_{27}	932 (5)	937 (14)	788 (6)	792 (6)	775 (7)	771 (6)
ν_{28}	793 (3)	799 (0)	747 (0)	748 (0)	744 (0)	745 (1)
ν_{29}	750 (0)	754 (1)	612 (1)	617 (1)	620 (2)	623 (2)
ν_{30}	618 (0)	625 (13)	509 (5)	514 (5)	503 (0)	508 (0)
ν_{31}	508 (0)	510 (3)	471 (1)	470 (0)	485 (0)	488 (0)
ν_{32}	494 (0)	494 (4)	345 (0)	349 (0)	346 (0)	351 (0)
ν_{33}	357 (4)	360 (3)	2888 (9)	2809 (12)	2857 (14)	2773 (19)
ν_{34}	945 (0)	976 (0)	1218 (1)	1206 (1)	1208 (1)	1195 (0)
ν_{35}	913 (2)	930 (0)	976 (1)	982 (0)	970 (11)	968 (8)
ν_{36}	902 (4)	913 (4)	971 (0)	999 (0)	964 (0)	992 (0)
ν_{37}	824 (0)	834 (0)	942 (3)	946 (3)	934 (0)	940 (0)
ν_{38}	761 (49)	760 (67)	914 (0)	912 (0)	906 (1)	906 (0)
ν_{39}	735 (77)	737 (17)	851 (1)	857 (0)	841 (1)	850 (1)
ν_{40}	712 (6)	713 (30)	772 (63)	773 (46)	748 (64)	752 (41)
ν_{41}	591 (4)	628 (2)	715 (7)	729 (22)	724 (10)	717 (16)
ν_{42}	571 (17)	550 (15)	699 (15)	698 (7)	670 (0)	667 (1)
ν_{43}	479 (16)	480 (20)	526 (0)	532 (1)	538 (6)	541 (5)
ν_{44}	428 (2)	430 (0)	462 (0)	469 (0)	452 (24)	454 (26)
ν_{45}	322 (28)	372 (32)	419 (10)	420 (11)	399 (2)	399 (2)
ν_{46}	279 (51)	451 (9)	238 (11)	241 (10)	236 (0)	242 (0)
ν_{47}	176 (10)	178 (6)	168 (0)	168 (1)	167 (0)	167 (0)
ν_{48}	148 (0)	152 (9)	65 (3)	78 (2)	101 (3)	110 (3)

[a] Harmonic vibrational wavenumbers scaled according to 0.9122 x + 174.3 for wavenumbers >2000 cm^{-1} and 0.9823 x + 0.6 for wavenumbers <2000 cm^{-1}. [b] IR intensities in km mol^{-1} are listed in parentheses.

Table S6 Scaled harmonic and anharmonic vibrational wavenumbers and IR intensities of 4-, 5-, and 6-*iso*-HC_9H_7N radicals calculated with the B3LYP/6-311++G(d,p) method

Mode	4-*iso*-HC_9H_7N		5-*iso*-HC_9H_7N		6-*iso*-HC_9H_7N	
	Scaled harm.[a]	Anharmonic	Scaled harm.[a]	Anharmonic	Scaled harm.[a]	Anharmonic
ν_{1}	3083 (18)	3041 (21)	3080 (16)	3082 (10)	3071 (20)	3054 (17)
ν_{2}	3070 (21)	3068 (24)	3070 (17)	3054 (15)	3067 (27)	3041 (29)
ν_{3}	3059 (7)	3096 (1)	3064 (26)	3038 (36)	3059 (10)	3032 (32)
ν_{4}	3055 (6)	2996 (29)	3054 (4)	3021 (14)	3048 (5)	2999 (3)
ν_{5}	3050 (7)	3003 (1)	3048 (4)	3007 (0)	3048 (14)	3017 (9)
ν_{6}	3026 (25)	3012 (24)	3031 (22)	2995 (10)	3030 (25)	3014 (10)
ν_{7}	2874 (29)	2832 (7)	2874 (26)	2841 (7)	2850 (39)	2808 (4)
ν_{8}	1598 (1)	1584 (0)	1582 (18)	1568 (10)	1639 (4)	1623 (3)
ν_{9}	1571 (1)	1562 (1)	1555 (9)	1546 (3)	1560 (25)	1550 (19)
ν_{10}	1511 (10)	1493 (5)	1522 (5)	1510 (4)	1515 (2)	1500 (1)
ν_{11}	1485 (11)	1477 (8)	1488 (2)	1481 (2)	1450 (22)	1440 (16)
ν_{12}	1446 (9)	1441 (4)	1426 (10)	1415 (5)	1431 (4)	1425 (2)
ν_{13}	1417 (11)	1398 (10)	1418 (14)	1396 (6)	1419 (11)	1420 (1)
ν_{14}	1372 (2)	1366 (0)	1406 (2)	1399 (1)	1406 (5)	1383 (7)
ν_{15}	1347 (1)	1341 (1)	1364 (1)	1358 (0)	1382 (5)	1378 (5)
ν_{16}	1314 (6)	1304 (5)	1310 (4)	1302 (3)	1337 (8)	1322 (8)
ν_{17}	1274 (10)	1270 (2)	1280 (5)	1273 (3)	1282 (13)	1282 (10)
ν_{18}	1249 (25)	1239 (21)	1252 (3)	1244 (2)	1259 (2)	1248 (0)
ν_{19}	1219 (5)	1213 (5)	1215 (3)	1212 (2)	1235 (1)	1235 (0)
ν_{20}	1184 (3)	1181 (2)	1202 (10)	1200 (9)	1185 (7)	1186 (4)
ν_{21}	1159 (0)	1164 (0)	1166 (1)	1162 (1)	1159 (4)	1158 (2)
ν_{22}	1138 (2)	1138 (2)	1156 (0)	1161 (0)	1155 (2)	1160 (3)
ν_{23}	1116 (0)	1112 (0)	1075 (2)	1078 (1)	1048 (5)	1047 (4)
ν_{24}	1034 (3)	1035 (2)	1052 (4)	1052 (3)	1030 (2)	1030 (1)
ν_{25}	941 (5)	941 (3)	938 (3)	937 (1)	918 (6)	917 (6)
ν_{26}	898 (4)	899 (3)	907 (6)	910 (5)	884 (21)	885 (19)
ν_{27}	783 (8)	785 (7)	790 (3)	788 (2)	776 (6)	775 (5)
ν_{28}	747 (1)	752 (1)	750 (3)	752 (3)	756 (1)	761 (1)
ν_{29}	618 (2)	622 (2)	622 (2)	624 (1)	622 (4)	624 (3)
ν_{30}	507 (1)	510 (1)	503 (0)	508 (0)	506 (0)	508 (0)
ν_{31}	477 (1)	479 (0)	473 (1)	474 (1)	484 (0)	484 (0)
ν_{32}	348 (0)	352 (0)	349 (0)	353 (0)	349 (0)	354 (0)
ν_{33}	2877 (11)	2794 (15)	2875 (11)	2797 (15)	2840 (13)	2755 (18)
ν_{34}	1168 (1)	1157 (0)	1183 (1)	1174 (0)	1162 (1)	1152 (0)
ν_{35}	972 (0)	993 (0)	958 (0)	969 (0)	979 (0)	980 (0)
ν_{36}	950 (1)	957 (1)	950 (1)	951 (2)	962 (0)	984 (0)
ν_{37}	923 (1)	930 (1)	928 (1)	934 (0)	920 (9)	931 (2)
ν_{38}	858 (1)	871 (1)	914 (2)	912 (2)	905 (9)	897 (13)
ν_{39}	782 (21)	816 (2)	823 (30)	825 (23)	812 (36)	815 (30)
ν_{40}	746 (64)	748 (65)	768 (1)	775 (6)	776 (3)	799 (2)
ν_{41}	716 (0)	722 (3)	710 (15)	709 (9)	698 (24)	700 (26)
ν_{42}	683 (0)	685 (0)	651 (45)	653 (39)	686 (6)	689 (4)
ν_{43}	524 (6)	530 (5)	546 (4)	546 (3)	547 (0)	550 (0)
ν_{44}	480 (6)	484 (6)	472 (7)	473 (7)	452 (21)	457 (23)
ν_{45}	424 (3)	428 (4)	403 (6)	403 (7)	370 (0)	376 (0)
ν_{46}	232 (3)	238 (3)	244 (2)	247 (2)	251 (2)	252 (1)
ν_{47}	167 (1)	168 (1)	169 (0)	168 (0)	170 (1)	172 (1)
ν_{48}	53 (2)	73 (2)	86 (0)	90 (0)	125 (0)	126 (0)

[a] Harmonic vibrational wavenumbers scaled according to $0.9122\, x + 174.3$ for wavenumbers >2000 cm^{-1} and $0.9823\, x + 0.6$ for wavenumbers <2000 cm^{-1}. [b] IR intensities in km mol^{-1} are listed in parentheses.

Table S7 Scaled harmonic and anharmonic vibrational wavenumbers and IR intensities of 7- and 8-*iso*-HC$_9$H$_7$N radicals calculated with the B3LYP/6-311++G(d,p) method

Mode	7-*iso*-HC$_9$H$_7$N		8-*iso*-HC$_9$H$_7$N	
	Scaled harm.[a]	Anharmonic	Scaled harm.[a]	Anharmonic
ν_{1}	3069 (27)	3028 (4)	3080 (16)	3092 (21)
ν_{2}	3065 (20)	3046 (19)	3070 (35)	3062 (4)
ν_{3}	3059 (17)	3044 (41)	3069 (2)	3025 (6)
ν_{4}	3053 (4)	3015 (6)	3053 (3)	3045 (15)
ν_{5}	3047 (3)	3063 (1)	3046 (17)	3007 (23)
ν_{6}	3028 (20)	3000 (12)	3024 (25)	2976 (12)
ν_{7}	2849 (48)	2759 (6)	2874 (20)	2838 (5)
ν_{8}	1641 (2)	1624 (0)	1585 (52)	1569 (32)
ν_{9}	1553 (35)	1541 (16)	1551 (4)	1540 (3)
ν_{10}	1512 (5)	1495 (1)	1527 (2)	1513 (1)
ν_{11}	1472 (3)	1466 (3)	1472 (14)	1464 (13)
ν_{12}	1435 (10)	1430 (3)	1431 (19)	1425 (4)
ν_{13}	1417 (6)	1392 (7)	1418 (7)	1400 (5)
ν_{14}	1407 (1)	1406 (3)	1409 (1)	1406 (3)
ν_{15}	1371 (5)	1368 (2)	1372 (1)	1365 (0)
ν_{16}	1334 (4)	1319 (4)	1314 (5)	1306 (3)
ν_{17}	1286 (10)	1283 (1)	1271 (9)	1269 (8)
ν_{18}	1257 (1)	1252 (0)	1259 (10)	1249 (7)
ν_{19}	1233 (0)	1231 (0)	1218 (4)	1215 (4)
ν_{20}	1208 (11)	1201 (5)	1184 (2)	1181 (3)
ν_{21}	1157 (0)	1160 (0)	1175 (4)	1174 (2)
ν_{22}	1141 (2)	1139 (2)	1158 (0)	1162 (0)
ν_{23}	1053 (2)	1054 (2)	1074 (2)	1076 (2)
ν_{24}	1016 (4)	1016 (3)	1057 (4)	1057 (2)
ν_{25}	914 (6)	914 (5)	935 (17)	937 (15)
ν_{26}	883 (12)	884 (11)	911 (5)	914 (4)
ν_{27}	777 (3)	776 (2)	787 (8)	786 (5)
ν_{28}	753 (2)	752 (2)	756 (0)	758 (0)
ν_{29}	627 (3)	630 (3)	621 (2)	624 (2)
ν_{30}	498 (2)	495 (1)	502 (2)	506 (2)
ν_{31}	488 (1)	490 (1)	475 (2)	475 (2)
ν_{32}	348 (0)	352 (0)	349 (0)	353 (0)
ν_{33}	2838 (15)	2753 (21)	2875 (10)	2796 (14)
ν_{34}	1166 (1)	1156 (1)	1179 (1)	1172 (0)
ν_{35}	980 (0)	985 (1)	972 (0)	984 (0)
ν_{36}	935 (3)	958 (1)	954 (1)	956 (2)
ν_{37}	912 (12)	911 (13)	942 (0)	950 (0)
ν_{38}	897 (0)	919 (1)	897 (1)	894 (1)
ν_{39}	821 (45)	828 (38)	834 (39)	835 (31)
ν_{40}	775 (2)	793 (1)	774 (1)	778 (3)
ν_{41}	694 (0)	714 (4)	716 (2)	720 (1)
ν_{42}	681 (13)	667 (7)	654 (43)	657 (38)
ν_{43}	554 (29)	557 (26)	549 (10)	544 (9)
ν_{44}	434 (7)	446 (10)	454 (0)	457 (0)
ν_{45}	381 (1)	387 (1)	410 (10)	415 (11)
ν_{46}	245 (0)	251 (0)	244 (1)	250 (1)
ν_{47}	168 (0)	170 (0)	170 (1)	170 (1)
ν_{48}	119 (1)	123 (1)	85 (1)	92 (1)

[a] Harmonic vibrational wavenumbers scaled according to $0.9122\,x + 174.3$ for wavenumbers >2000 cm^{-1} and $0.9823\,x + 0.6$ for wavenumbers <2000 cm^{-1}. [b] IR intensities in km mol^{-1} are listed in parentheses.

Table S8 Scaled harmonic and anharmonic vibrational wavenumbers and IR intensities of 4a- and 8a-*iso*-HC_9H_7N radicals calculated with the B3LYP/6-311++G(d,p) method

Mode	4a-*iso*-HC_9H_7N		8a-*iso*-HC_9H_7N	
	Scaled harm.[a]	Anharmonic	Scaled harm.[a]	Anharmonic
ν_1	3084 (13)	3062 (2)	3084 (12)	3021 (18)
ν_2	3072 (40)	3050 (38)	3081 (20)	3060 (50)
ν_3	3071 (11)	3029 (13)	3069 (22)	3064 (9)
ν_4	3056 (2)	3028 (13)	3056 (8)	3041 (7)
ν_5	3053 (7)	3039 (8)	3054 (1)	3068 (15)
ν_6	3051 (7)	3001 (9)	3051 (5)	3011 (1)
ν_7	3013 (23)	2983 (25)	3010 (18)	2987 (19)
ν_8	2631 (16)	2498 (5)	2653 (24)	2526 (19)
ν_9	1594 (5)	1577 (2)	1597 (1)	1583 (1)
ν_{10}	1585 (24)	1569 (10)	1585 (29)	1564 (6)
ν_{11}	1482 (1)	1467 (1)	1488 (1)	1475 (1)
ν_{12}	1466 (10)	1456 (6)	1473 (2)	1463 (1)
ν_{13}	1400 (6)	1394 (1)	1430 (0)	1425 (0)
ν_{14}	1395 (4)	1386 (4)	1385 (2)	1382 (1)
ν_{15}	1370 (4)	1366 (2)	1360 (1)	1357 (0)
ν_{16}	1332 (5)	1315 (4)	1318 (3)	1309 (2)
ν_{17}	1287 (0)	1277 (0)	1300 (1)	1291 (0)
ν_{18}	1240 (19)	1238 (3)	1249 (5)	1254 (1)
ν_{19}	1225 (1)	1223 (0)	1228 (11)	1223 (7)
ν_{20}	1186 (7)	1186 (2)	1198 (14)	1188 (4)
ν_{21}	1171 (5)	1159 (4)	1160 (2)	1162 (1)
ν_{22}	1153 (0)	1154 (0)	1153 (3)	1150 (3)
ν_{23}	1102 (11)	1099 (7)	1087 (14)	1086 (8)
ν_{24}	1064 (8)	1057 (5)	1063 (3)	1058 (3)
ν_{25}	1059 (1)	1054 (1)	1052 (2)	1046 (1)
ν_{26}	988 (4)	984 (2)	989 (4)	989 (3)
ν_{27}	980 (4)	979 (4)	980 (6)	977 (7)
ν_{28}	963 (1)	960 (1)	957 (1)	961 (1)
ν_{29}	961 (2)	963 (0)	936 (5)	936 (5)
ν_{30}	942 (5)	940 (4)	910 (1)	906 (0)
ν_{31}	909 (6)	923 (12)	903 (3)	898 (3)
ν_{32}	906 (11)	896 (0)	892 (2)	889 (1)
ν_{33}	840 (17)	837 (20)	796 (45)	796 (24)
ν_{34}	784 (22)	785 (9)	793 (2)	791 (7)
ν_{35}	763 (14)	766 (11)	770 (10)	774 (5)
ν_{36}	726 (14)	725 (24)	738 (5)	736 (8)
ν_{37}	687 (42)	696 (13)	685 (48)	686 (37)
ν_{38}	670 (0)	662 (8)	667 (4)	667 (4)
ν_{39}	620 (3)	624 (2)	614 (4)	618 (4)
ν_{40}	562 (11)	563 (10)	562 (7)	564 (7)
ν_{41}	510 (4)	511 (3)	509 (1)	511 (1)
ν_{42}	465 (8)	467 (8)	473 (8)	478 (1)
ν_{43}	451 (8)	451 (8)	464 (9)	461 (13)
ν_{44}	436 (6)	437 (6)	421 (9)	421 (1)
ν_{45}	342 (1)	342 (1)	346 (1)	345 (1)
ν_{46}	314 (1)	318 (1)	313 (20)	316 (0)
ν_{47}	150 (0)	150 (0)	150 (0)	150 (0)
ν_{48}	117 (1)	118 (1)	111 (0)	111 (0)

[a] Harmonic vibrational wavenumbers scaled according to $0.9122\,x + 174.3$ for wavenumbers >2000 cm^{-1} and $0.9823\,x + 0.6$ for wavenumbers <2000 cm^{-1}. [b] The IR intensities in km mol^{-1} are listed in parentheses.

Table S9 Comparison of observed vibrational wavenumbers (in cm^{-1}) and relative IR intensities of isoquinoline (*iso*-C_9H_7N) with scaled harmonic and anharmonic vibrational wavenumbers and IR intensities predicted with the B3LYP/6-311++G(d,p)

Mode	Sym.	Calculations				Experiment	
		Scaled harmonic[a]		Anharmonic		p-H_2	
ν_1	a'	3083	(15)[b]	3066	(21)[b]	3069.6	(64)[c]
ν_2	a'	3074	(42)	3036	(22)	3033.3	(9)
ν_3	a'	3072	(6)	3068	(29)		
ν_4	a'	3062	(1)	3047	(4)		
ν_5	a'	3057	(1)	3028	(2)		
ν_6	a'	3055	(7)	3000	(6)		
ν_7	a'	3023	(20)	3002	(9)	2992.3	(10)
ν_8	a'	1635	(22)	1622	(16)	1632.8	(50)
ν_9	a'	1595	(19)	1587	(11)	1595.0	(41)
ν_{10}	a'	1578	(7)	1574	(5)	1579.0	(15)
ν_{11}	a'	1507	(10)	1499	(9)	1502.1	(20)
ν_{12}	a'	1463	(1)	1462	(1)		
ν_{13}	a'	1439	(1)	1433	(1)		
ν_{14}	a'	1385	(6)	1385	(4)	1384.8	(8)
ν_{15}	a'	1376	(5)	1363	(4)	1379.1	(12)
ν_{16}	a'	1341	(0)	1335	(0)		
ν_{17}	a'	1267	(16)	1265	(13)	1273.0	(23)
ν_{18}	a'	1256	(1)	1257	(1)		
ν_{19}	a'	1220	(6)	1219	(2)	1220.7	(5)
ν_{20}	a'	1184	(1)	1187	(1)		
ν_{21}	a'	1148	(2)	1150	(2)		
ν_{22}	a'	1140	(2)	1143	(0)		
ν_{23}	a'	1044	(4)	1046	(1)	1036.6	(5)
ν_{24}	a'	1019	(5)	1019	(4)		
ν_{25}	a'	940	(8)	944	(9)	945.1	(19)
ν_{26}	a'	799	(3)	801	(4)	800.2	(10)
ν_{27}	a'	777	(1)	779	(1)	782.2	(2)
ν_{28}	a'	644	(5)	649	(5)	640.2	(11)
ν_{29}	a'	522	(0)	525	(0)		
ν_{30}	a'	502	(1)	506	(1)		
ν_{31}	a'	356	(0)	361	(0)		
ν_{32}	a'	984	(0)	995	(0)		
ν_{33}	a'	971	(1)	996	(0)		
ν_{34}	a''	957	(2)	967	(2)	954.6	(3)
ν_{35}	a''	927	(1)	946	(0)	930.2	(2)
ν_{36}	a''	860	(9)	869	(8)	860.6	(15)
ν_{37}	a''	829	(51)	830	(41)	826.3	(100)
ν_{38}	a''	774	(1)	791	(0)	778.5	(3)
ν_{39}	a''	740	(32)	741	(29)	740.1	(63)
ν_{40}	a''	640	(5)	642	(4)	636.3	(11)
ν_{41}	a''	484	(20)	487	(25)	481.0	(30)
ν_{42}	a''	460	(1)	466	(1)		
ν_{43}	a''	379	(0)	383	(0)		
ν_{44}	a''	182	(1)	182	(1)		
ν_{45}	a''	169	(0)	168	(0)		

[a] Harmonic vibrational wavenumbers scaled according to $0.9122x + 174.3$ for wavenumbers >2000 cm^{-1} and $0.9823\,x + 0.6$ for wavenumbers <2000 cm^{-1}. [b] IR intensities in km mol^{-1} are listed in parentheses. [c] IR intensities as per cent of that of the line at 826.3 cm^{-1} are listed in parentheses.

Table S10 Summary of the estimation of mixing ratios of each species in the UV/IR irradiated *iso*-C_9H_7N/Cl_2/*p*-H_2 matrix experiments

Group	Assignments	Mixing ratio	Lines (cm^{-1}) integrated
parent	*iso*-C_9H_7N	(90 ± 12) ppm	1632.8, 1273.0, 826.3, 741.1, and 945.1
A	*iso*-C_9H_7NH	(2.8 ± 0.5) ppm	3495.2, 1420.7, 763.1, and 737.3
B	6-*iso*-HC_9H_7N	(2.1 ± 1.2) ppm	1557.5, 1446.8, 1284.5, and 810.2
C	7-*iso*HC_9H_7N	(1.1 ± 0.4) ppm	1551.2, 1205.1, and 908.4
D	8-*iso*-HC_9H_7N	(1.6 ± 0.1) ppm	1467.6, 830.5, and 653.7
E	4-*iso*-HC_9H_7N	(2.5 ± 0.3) ppm	1483.7, 1269.4, 1245.9, and 748.1
F	5-*iso*-HC_9H_7N	(1.5 ± 0.3) ppm	1201.3, 821.9, 708.6, and 652.3
G	1-*iso*-HC_9H_7N	(1.5 ± 0.3) ppm	1416.6, 918.3, 769.2, and 714.6
H	3-*iso*-HC_9H_7N	(0.42 ± 0.01) ppm	1642.7 and 876.4

Table S11 Vertical excitation wavelengths and oscillator strengths of electronic excitation of *iso*-C_9H_7NH, 1-*iso*-HC_9H_7N, *iso*-C_9H_7NH, and 3-*iso*-HC_9H_7N predicted with the TD-B3LYP/6-311++G(d,p) method

State	*iso*-C_9H_7N			1-*iso*-HC_9H_7N			*iso*-C_9H_7NH			3-*iso*-HC_9H_7N		
	λ /nm	*f* /10^{-1}	Assignment	λ /nm	*f* /10^{-2}	Assignment	λ /nm	*f* /10^{-2}	Assignment	λ /nm	*f* /10^{-2}	Assignment
1	291	0.1	HOMO – 1 → LUMO	536	0.1	HOMO(β) → LUMO(β)	844	0.1	HOMO(□) → LUMO (□)	520	0.4	HOMO(□) → LUMO (□)
2	288	5.6	HOMO → LUMO	424	0.1	HOMO – 2(β) → LUMO(β)	585	0.1	HOMO(□) → LUMO + 1(□)	412	0.0	HOMO(β) → LUMO (β)
3	268	1.4	HOMO – 2 → LUMO	405	0.2	HOMO – 1(β) → LUMO(β)	483	3.1	HOMO(□) → LUMO + 4(□)	376	0.4	HOMO(□) → LUMO + 2(□)
4	246	0.0	HOMO → LUMO + 2	347	1.5	HOMO(□) → LUMO + 2(□)	430	0.0	HOMO(□) → LUMO + 3(□)	367	4.2	HOMO – 1 (β) → LUMO (β)
5	222	0.0	HOMO → LUMO + 3	322	20.1	HOMO – 2(β) → LUMO(β)	426	0.2	HOMO(□) → LUMO + 2(□)	332	0.4	HOMO – 1(β) → LUMO + 1(β)
6	221	0.5	HOMO → LUMO + 4	302	0.5	HOMO – 2(□) → LUMO + 1(□)	371	1.8	HOMO(β) → LUMO(β)	316	0.0	HOMO – 1(□) → LUMO(□)
7	210	0.0	HOMO → LUMO + 5	285	0.4	HOMO(□) → LUMO + 2(□)	366	0.1	HOMO(□) → LUMO + 5(□)	312	0.0	HOMO(□) → LUMO + 1(□)
8	207	10.5	HOMO – 2 → LUMO	280	0.3	HOMO – 3(β) → LUMO(β)	357	0.1	HOMO(□) → LUMO + 6(□)	298	3.7	HOMO – 2(β) → LUMO(β)
9	204	0.5	HOMO – 2 → LUMO + 2	265	0.1	HOMO(□) → LUMO + 3(□)	332	4.2	HOMO(β) → LUMO + 1(β)	287	0.1	HOMO(□) → LUMO + 3(□)
10	204	0.1	HOMO – 1 → LUMO + 6	262	0.0	HOMO – 1(□) → LUMO(□)	324	0.5	HOMO(□) → LUMO + 8(□)	279	0.2	HOMO(β) → LUMO + 1(β)
11	203	0.1	HOMO – 2 → LUMO +2	259	0.1	HOMO(□) → LUMO + 4(□)	316	0.1	HOMO(□) → LUMO + 10(□)	275	0.0	HOMO(□) → LUMO + 4(□)
12	198	1.3	HOMO – 2 → LUMO +2	249	0.1	HOMO – 2(□) → LUMO(□)	308	0.1	HOMO(□) → LUMO + 11(□)	263	3.9	HOMO(□) → LUMO + 5(□)

Table S12 Vertical excitation wavelengths and oscillator strengths of electronic excitation of 4-*iso*-HC$_9$H$_7$N, 4a-*iso*-HC$_9$H$_7$N, 5-*iso*-HC$_9$H$_7$N, and 6-*iso*-HC$_9$H$_7$N predicted with the TD-B3LYP/6-311++G(d,p) method

State	4-*iso*-HC$_9$H$_7$N			4a-*iso*-HC$_9$H$_7$N			5-*iso*-HC$_9$H$_7$N			6-*iso*-HC$_9$H$_7$N		
	λ /nm	*f* /10^{-2}	Assignment	λ /nm	*f* /10^{-2}	Assignment	λ /nm	*f* /10^{-2}	Assignment	λ /nm	*f* /10^{-2}	Assignment
1	450	2.5	HOMO(□) → LUMO(□)	618	0.3	HOMO(β) → LUMO(β)	452	0.5	HOMO(□) → LUMO(□)	504	0.6	HOMO(β) → LUMO(β)
2	406	0.0	HOMO(β) → LUMO(β)	497	0.3	HOMO – 1(β) → LUMO(β)	417	0.3	HOMO(□) → LUMO + 1(□)	443	0.0	HOMO – 1(β) → LUMO(β)
3	397	0.4	HOMO(□) → LUMO + 1(□)	463	6.8	HOMO(□) → LUMO(□)	352	0.0	HOMO – 1(β) → LUMO(β)	407	4.7	HOMO(□) → LUMO(□)
4	342	1.4	HOMO – 1(β) → LUMO(β)	405	2.5	HOMO – 2(β)→ LUMO(β)	330	18.6	HOMO(β) → LUMO(β)	358	0.7	HOMO(□) → LUMO +2(□)
5	324	11.6	HOMO – 2(β) → LUMO(β)	362	0.2	HOMO – 2(β) → LUMO(β)	320	0.0	HOMO(□) → LUMO +2(□)	342	0.3	HOMO(β) → LUMO + 1(β)
6	312	0.1	HOMO(□) → LUMO + 2(□)	324	1.9	HOMO(□) → LUMO + 1(□)	305	1.4	HOMO – 2(β) → LUMO(β)	307	0.0	HOMO(□) → LUMO + 1(□)
7	296	4.7	HOMO – 2(□) → LUMO + 1(□)	304	0.2	HOMO(□) → LUMO +2(□)	298	0.0	HOMO – 1(□) → LUMO(□)	288	2.0	HOMO(□) → LUMO + 2(□)
8	289	0.1	HOMO – 1(□) → LUMO(□)	303	0.0	HOMO – 2(β) → LUMO + 1(β)	298	1.2	HOMO – 2(β) → LUMO(β)	280	0.7	HOMO – 3(β) → LUMO(β)
9	285	0.1	HOMO(□) → LUMO + 3(□)	291	0.2	HOMO – 1(□) → LUMO(□)	286	0.0	HOMO(□) → LUMO + 3(□)	271	0.0	HOMO(□) → LUMO + 3(□)
10	275	0.1	HOMO(□) → LUMO + 4(□)	278	0.0	HOMO(□) → LUMO + 3(□)	276	0.6	HOMO – 2(□) → LUMO(□)	266	0.0	HOMO – 2(□) → LUMO(□)
11	269	2.2	HOMO(□) → LUMO +8(□)	276	0.7	HOMO – 2(β) → LUMO + 1(β)	275	0.3	HOMO(□) → LUMO + 4(□)	260	0.0	HOMO(□) → LUMO + 4(□)
12	251	0.5	HOMO – 2(□) → LUMO(□)	272	1.1	HOMO(□) → LUMO + 4(□)	254	0.4	HOMO – 1(β) → LUMO + 1(β)	259	0.0	HOMO – 1(β) → LUMO + 1(β)

Table S13 Vertical excitation wavelengths and oscillator strengths of electronic excitation of 7-*iso*-HC_9H_7N, 8-*iso*-HC_9H_7N, and 8a-*iso*-HC_9H_7N predicted with the TD-B3LYP/6-311++G(d,p) method

State	7-*iso*-HC_9H_7N			8-*iso*-HC_9H_7N			8a-*iso*-HC_9H_7N		
	λ /nm	*f* $/10^{-2}$	Assignment	λ /nm	*f* $/10^{-2}$	Assignment	λ /nm	*f* $/10^{-2}$	Assignment
1	544	0.7	HOMO(□) → LUMO(□)	437	0.6	HOMO(□) → LUMO(□)	632	0.2	HOMO(□) → LUMO(□)
2	378	1.6	HOMO(β) → LUMO(β)	400	0.0	HOMO(β) → LUMO(β)	465	7.0	HOMO(β) → LUMO(β)
3	374	2.7	HOMO(β) → LUMO(β)	388	0.3	HOMO – 1(β) → LUMO(β)	416	0.4	HOMO(□) → LUMO + 1(□)
4	373	0.0	HOMO – 1(β) → LUMO(β)	348	2.2	HOMO(□) → LUMO + 1(□)	383	3.9	HOMO – 1(β) → LUMO(β)
5	335	1.7	HOMO(β) → LUMO + 1(β)	322	15.8	HOMO – 2(β) → LUMO(β)	371	0.7	HOMO(□) → LUMO + 1(□)
6	325	0.0	HOMO(□) → LUMO + 2(□)	307	0.0	HOMO(□) → LUMO + 2(□)	318	0.3	HOMO(□) → LUMO + 2(□)
7	318	0.0	HOMO – 1(□) → LUMO(□)	304	1.4	HOMO – 2(□) → LUMO + 1(□)	312	0.3	HOMO – 2(□) → LUMO(□)
8	295	1.5	HOMO – 2(β) → LUMO(β)	277	0.0	HOMO(□) → LUMO + 3(□)	308	0.9	HOMO – 2(β) → LUMO(β)
9	287	0.0	HOMO(□) → LUMO + 3(□)	273	0.9	HOMO – 3(β) → LUMO(β)	293	0.1	HOMO – 2(□) → LUMO + 1(□)
10	278	0.1	HOMO(□) → LUMO + 4(□)	270	0.0	HOMO – 1(□) → LUMO(□)	287	0.1	HOMO(□) → LUMO + 3(□)
11	271	3.9	HOMO(□) → LUMO + 5(□)	264	0.1	HOMO(□) → LUMO + 4(□)	285	0.5	HOMO(□) → LUMO + 3(□)

12	269	0.2	HOMO – 1(β) → LUMO + 1(β)	255	0.4	HOMO – 2(□) → LUMO(□)	275	6.5	HOMO – 1(β) → LUMO + 1(β)

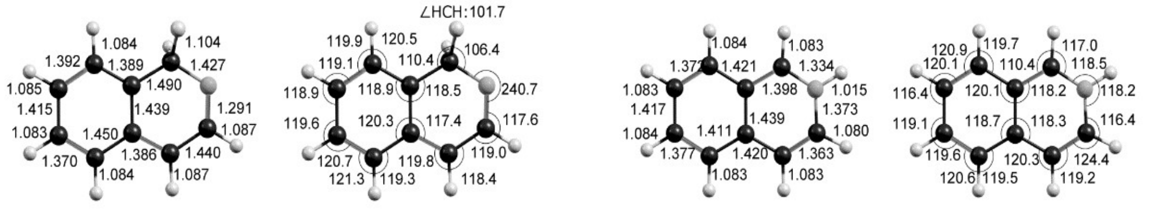
(a) 1-*iso*-H$^+$C$_9$H$_7$N, 200 kJ mol^{-1}

(b) *iso*-C$_9$H$_7$NH$^+$, 0 kJ mol^{-1}

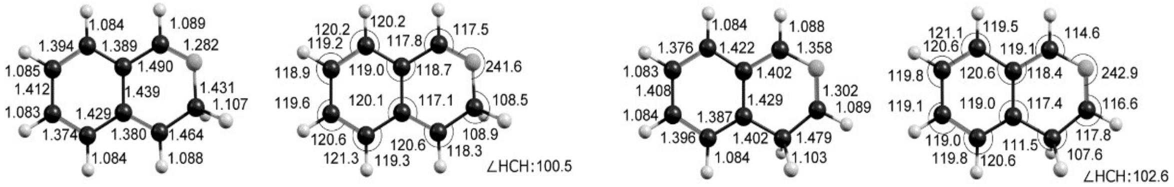
(c) 3-*iso*-H$^+$C$_9$H$_7$N, 190 kJ mol^{-1}

(d) 4-*iso*-H$^+$C$_9$H$_7$N, 169 kJ mol^{-1}

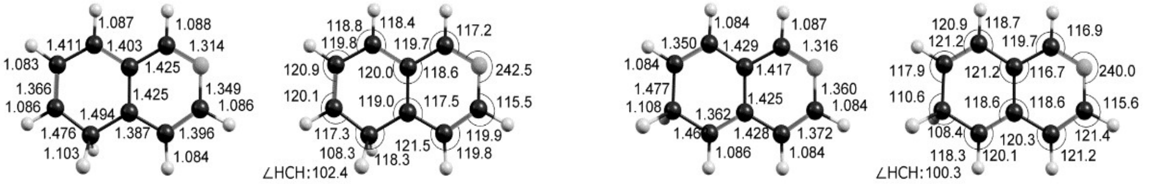
(e) 5-*iso*-H$^+$C$_9$H$_7$N, 171 kJ mol^{-1}

(f) 6-*iso*-H$^+$C$_9$H$_7$N, 209 kJ mol^{-1}

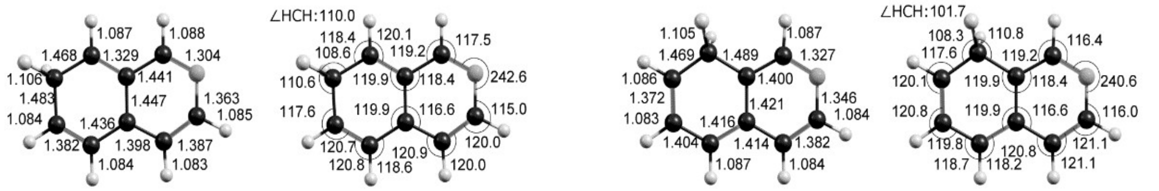
(g) 7-*iso*-H$^+$C$_9$H$_7$N, 183 kJ mol^{-1}

(h) 8-*iso*-H$^+$C$_9$H$_7$N, 190 kJ mol^{-1}

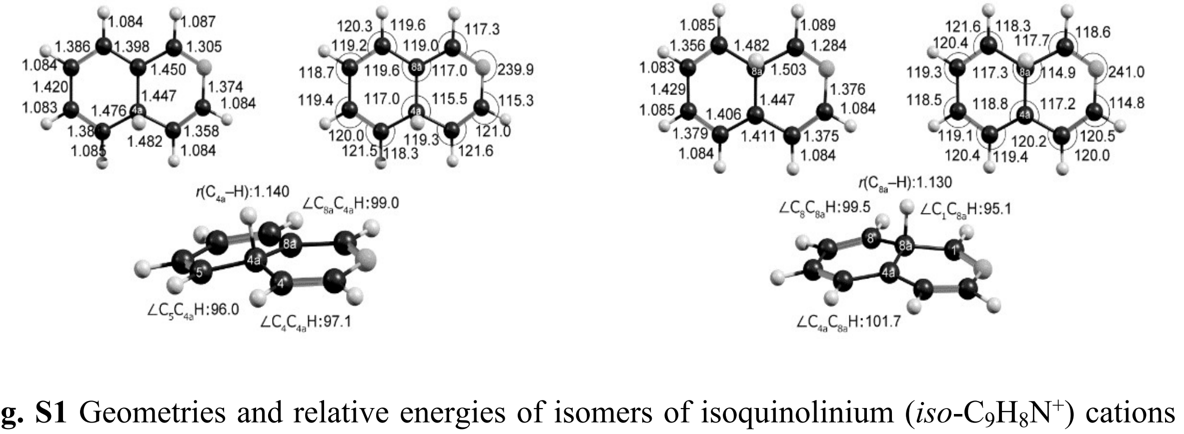
(i) 4a-*iso*-H$^+$C$_9$H$_7$N, 267 kJ mol^{-1}

(j) 8a-*iso*-H$^+$C$_9$H$_7$N, 240 kJ mol^{-1}

Fig. S1 Geometries and relative energies of isomers of isoquinolinium (*iso*-C$_9$H$_8$N$^+$) cations calculated with the CCSD(T)/6-311++G(d,p)//B3LYP/6-311++G(d,p) method. Energies were corrected for ZPVE calculated with the B3LYP/6-311++G(d,p) method. Bond lengths are in Å and bond angles in degree.

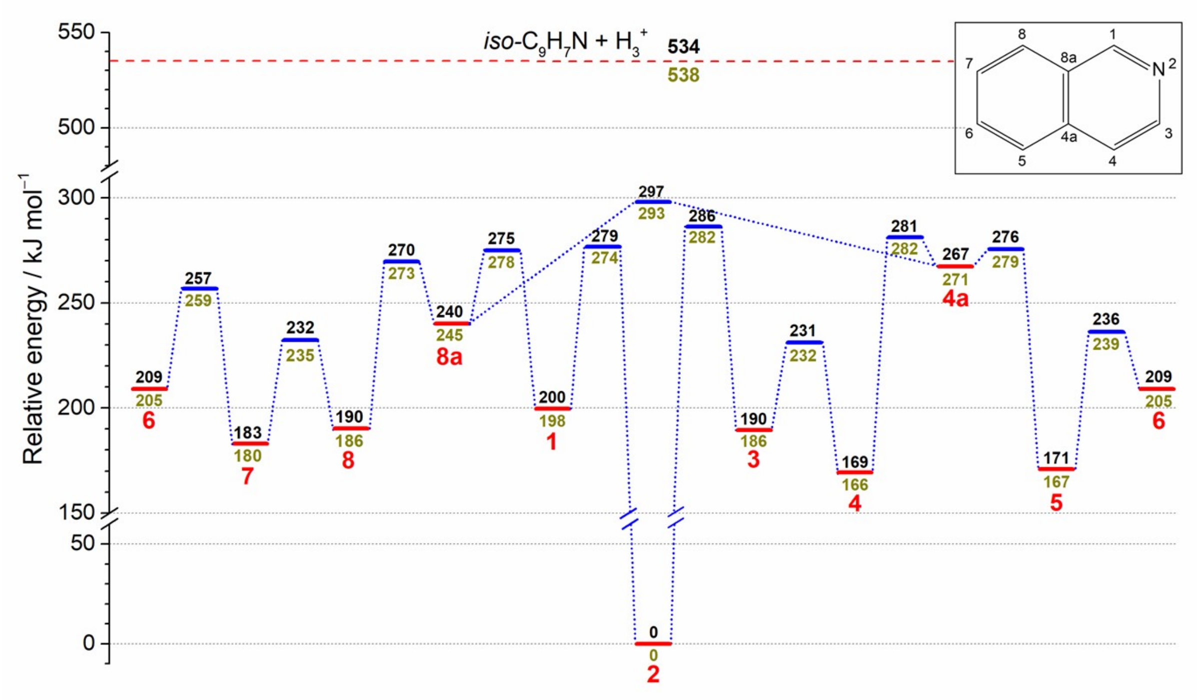

Fig. S2 Potential-energy scheme for isomerization among various isomers of isoquinolinium (iso-C$_9$H$_8$N$^+$) cations. The isomers (in red) are indicated by the site-number of protonation (see upper-right inset for the numbering), and transition states connecting them are in blue. The energies relative to the most stable isomer iso-C$_9$H$_7$NH$^+$ (2), calculated with the CCSD(T)/6-311++G(d,p)//B3LYP/6-311++G(d,p) method, are in black; values calculated with the B3LYP/6-311++G(d,p) method are in olive. ZPVE obtained from the B3LYP/6-311++G(d,p) method were corrected.

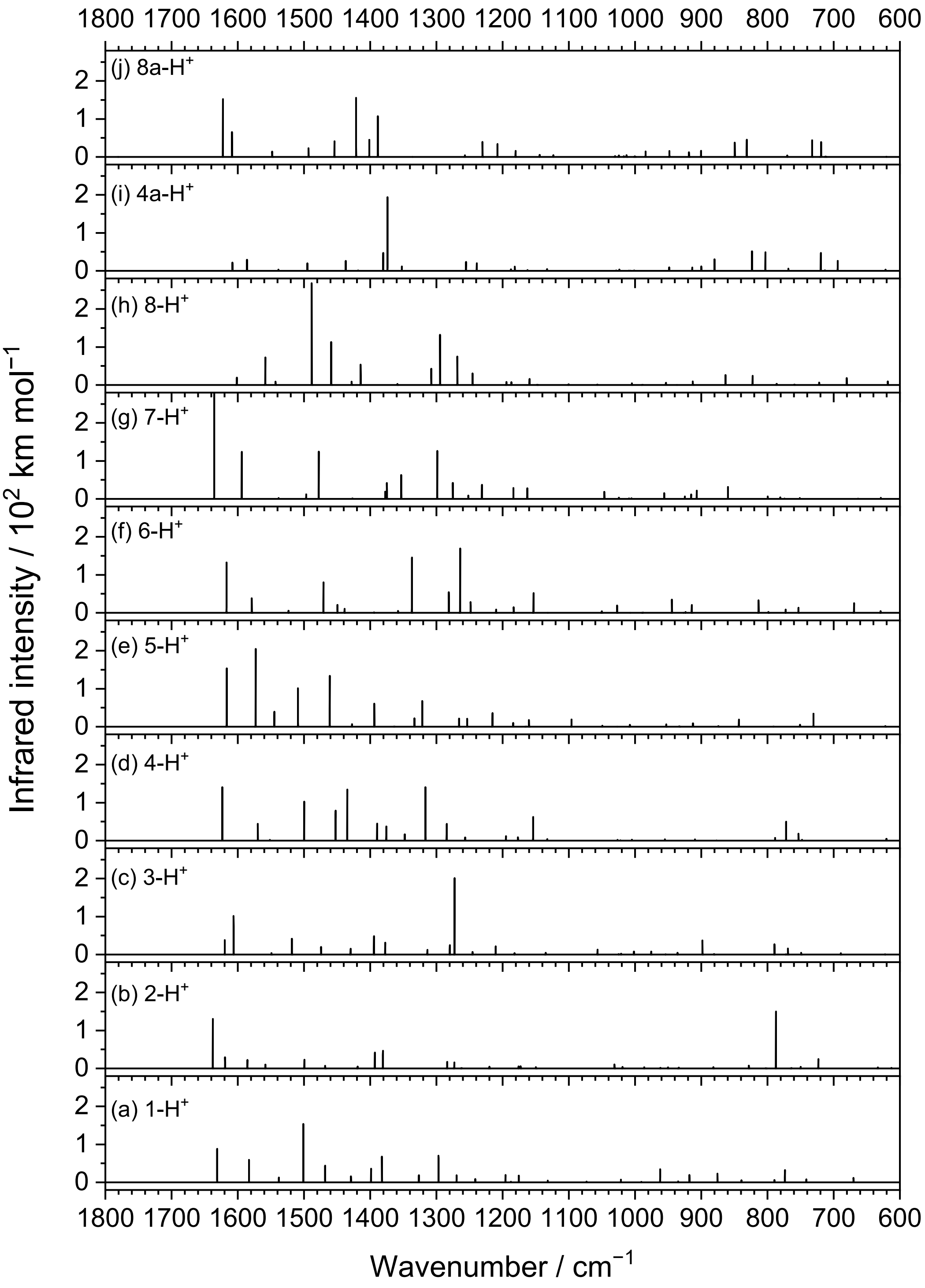

Fig. S3 Predicted IR spectra of all isomers of protonated isoquinoline simulated according to scaled harmonic vibrational wavenumbers and IR intensities calculated with the B3LYP/6-311++G(d,p) method. The label *n*-H$^+$ refers to *n*-isoquinolinium cation (*n*-H$^+$C$_9$H$_7$N).

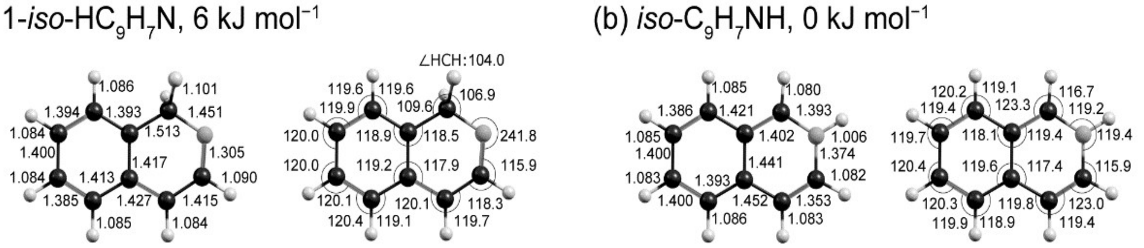
(a) 1-*iso*-HC_9H_7N, 6 kJ mol^{-1}

(b) *iso*-C_9H_7NH, 0 kJ mol^{-1}

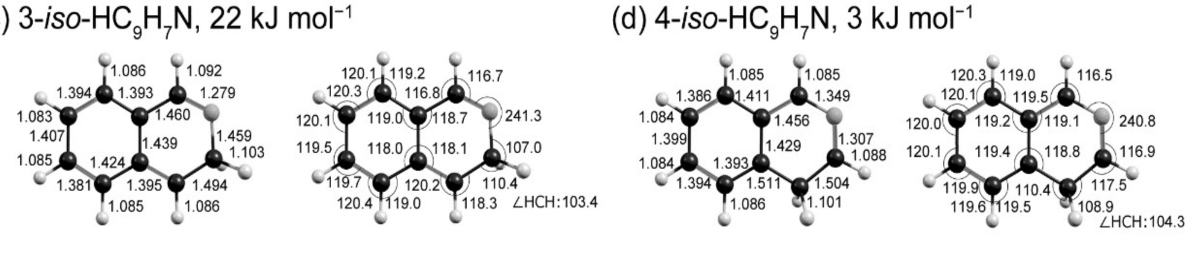
(c) 3-*iso*-HC_9H_7N, 22 kJ mol^{-1}

(d) 4-*iso*-HC_9H_7N, 3 kJ mol^{-1}

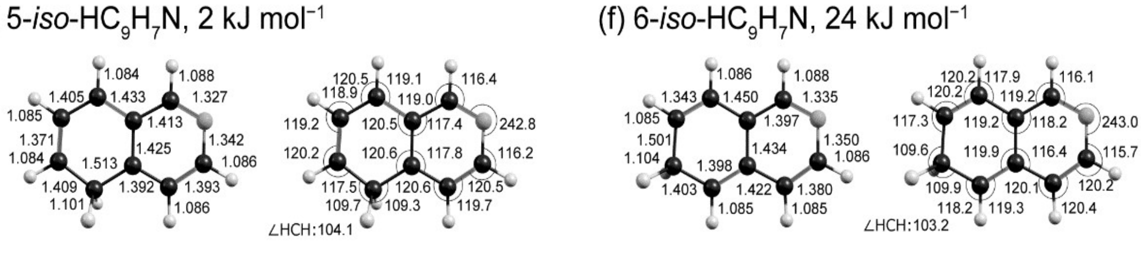
(e) 5-*iso*-HC_9H_7N, 2 kJ mol^{-1}

(f) 6-*iso*-HC_9H_7N, 24 kJ mol^{-1}

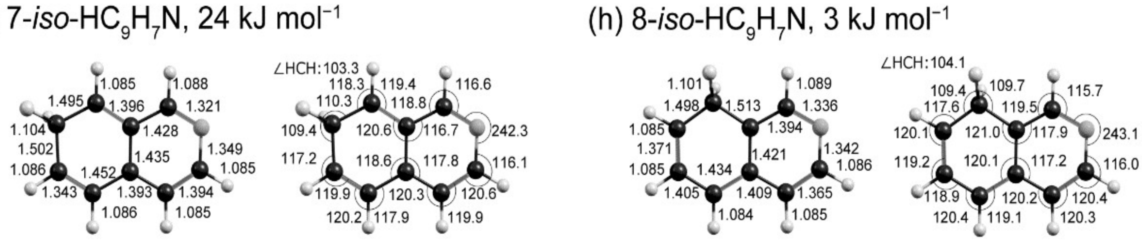
(g) 7-*iso*-HC_9H_7N, 24 kJ mol^{-1}

(h) 8-*iso*-HC_9H_7N, 3 kJ mol^{-1}

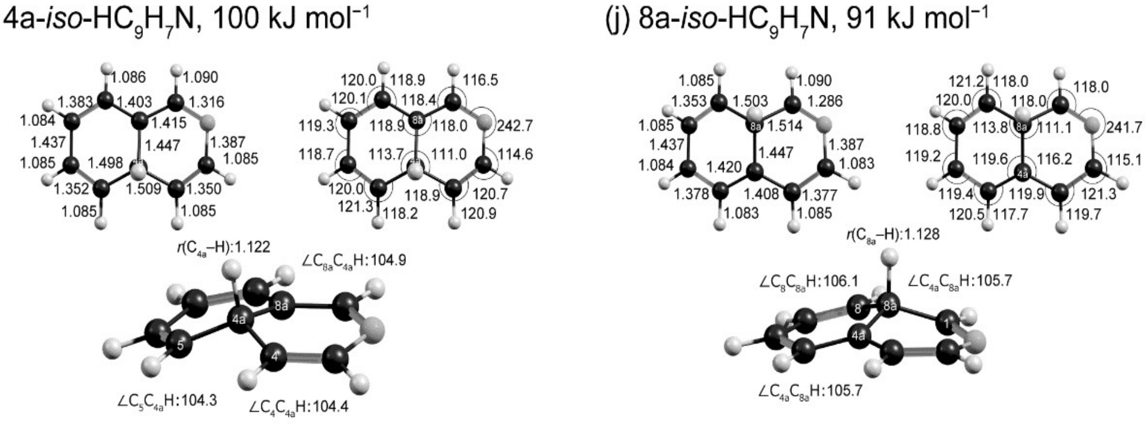
(i) 4a-*iso*-HC_9H_7N, 100 kJ mol^{-1}

(j) 8a-*iso*-HC_9H_7N, 91 kJ mol^{-1}

Fig. S4 Geometries and relative energies of isomers of isoquinolinyl (*iso*-C_9H_8N) radicals calculated with the CCSD(T)/6-311++G(d,p)//B3LYP/6-311++G(d,p) method. Energies were corrected for ZPVE calculated with the B3LYP/6-311++G(d,p) method. Bond lengths are in Å and bond angles in degree.

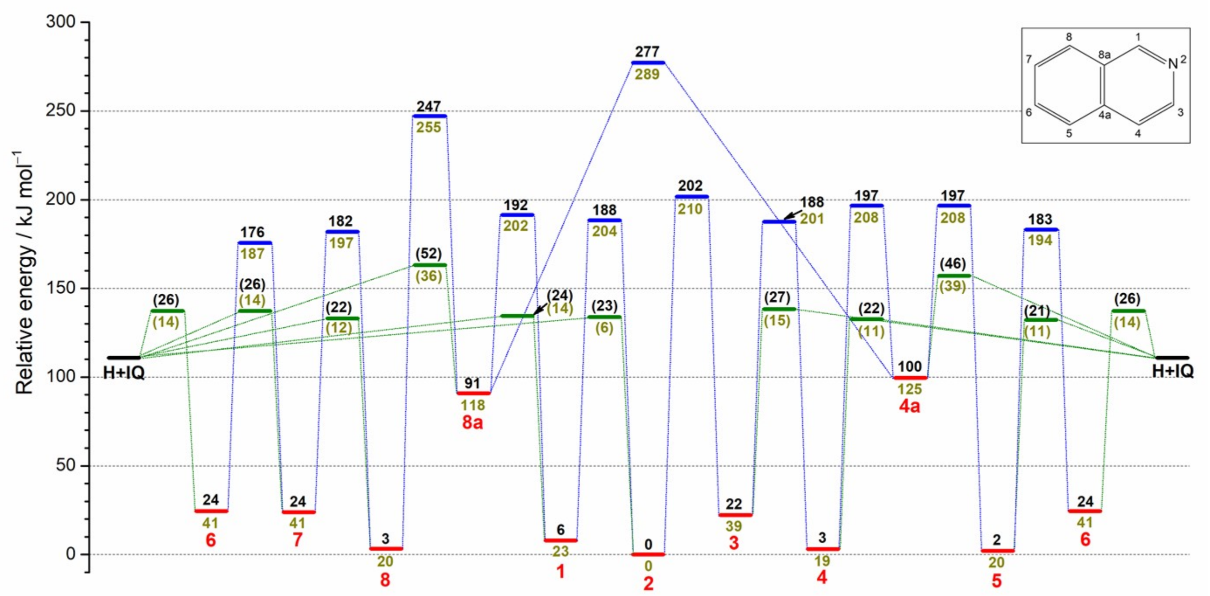

Fig. S5 Potential-energy scheme for the formation and isomerization of various isomers of isoquinolinyl (*iso*-C_9H_7N, indicated as IQ) radicals. The isomers (in red) are indicated by the site-number of hydrogenation (see upper-right inset for the numbering). Transition states for isomerization are in blue and those for the formation from H + *iso*-C_9H_7N are in green. The energies relative to the most stable isomer *iso*-C_9H_7NH (2), calculated with the CCSD(T)/6-311++G(d,p)//B3LYP/6-311++G(d,p) method, are in black; values calculated with the B3LYP/6-311++G(d,p) method are in olive. ZPVE obtained from the B3LYP/6-311++G(d,p) method were corrected. The energy of H + *iso*-C_9H_7N is 111 or 147 kJ mol^{-1} above *iso*-C_9H_7NH according to CCSD(T) or B3LYP calculations, respectively.

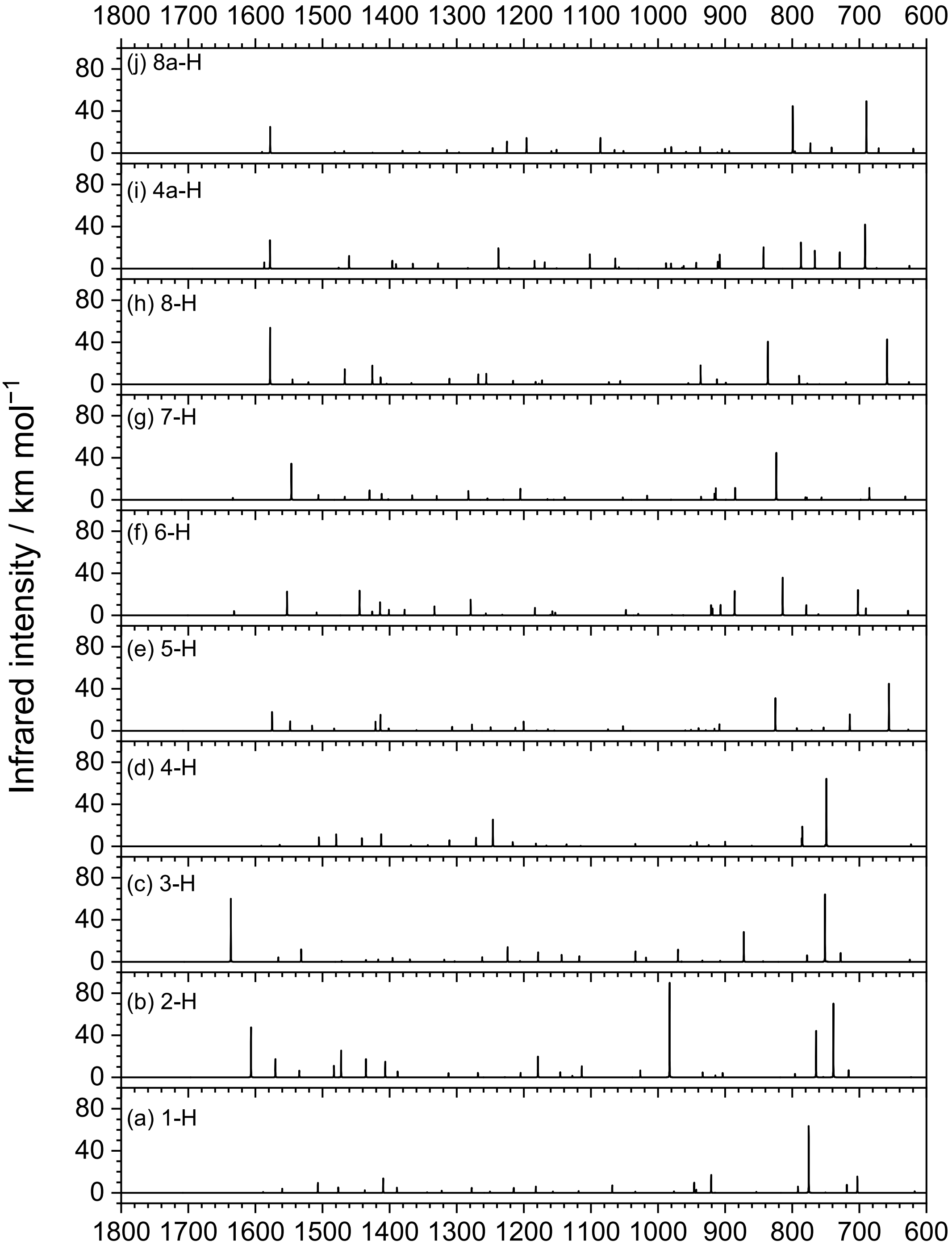

Fig. S6 Predicted IR spectra of all isomers of hydrogenated isoquinoline simulated according to scaled harmonic wavenumbers and IR intensities calculated with the B3LYP /6-311++G(d,p) method. The label *n*-H refers to *n*-isoquinolinyl radical (*n*-*iso*-HC_9H_7N).

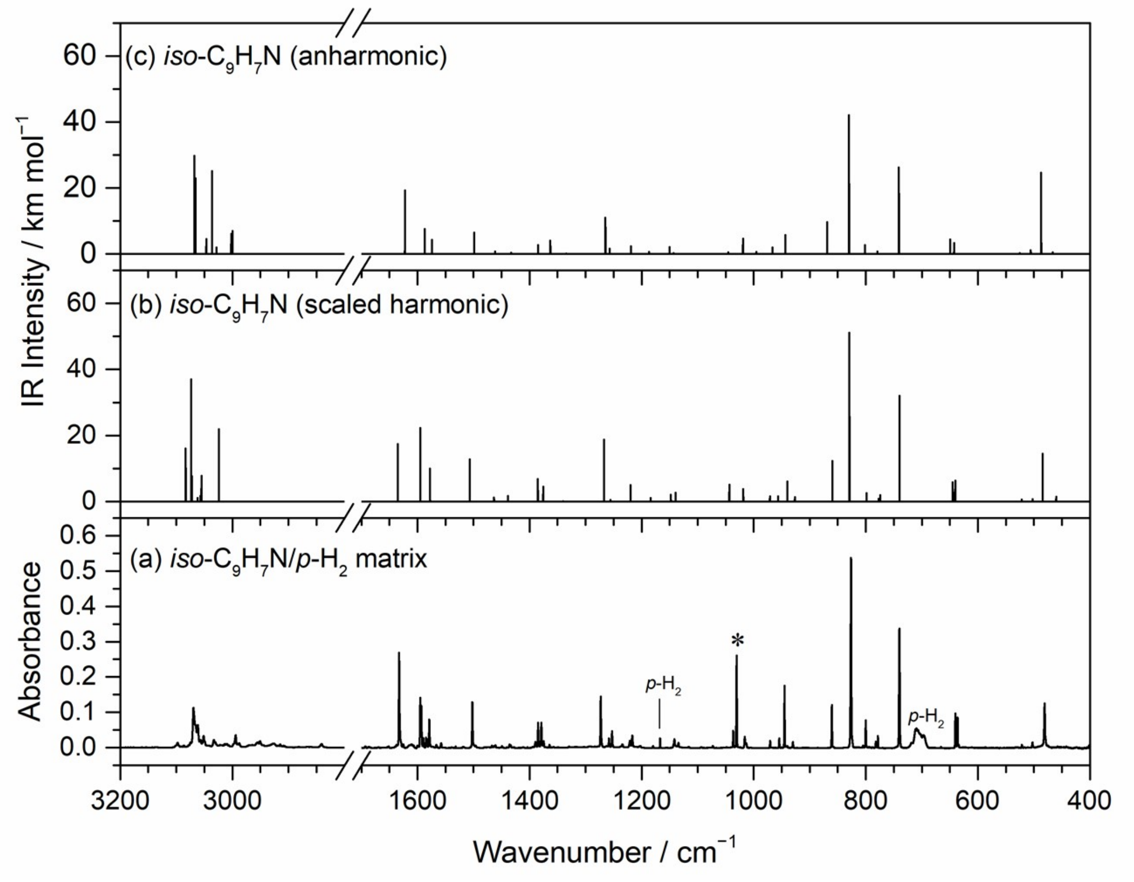

Fig. S7 Comparison of experimental and predicted IR spectra of *iso*-C_9H_7N. (a) Experimental absorption spectrum of an *iso*-C_9H_7N/*p*-H_2 matrix. Absorptions near 700 cm^{-1} and at 1167.0 cm^{-1} originate from solid *p*-H_2. A line at 1030.6 cm^{-1} (marked with *) is due to an impurity. (b) Simulated stick spectrum of *iso*-C_9H_7N according to scaled harmonic vibrational wavenumbers and IR intensities predicted with the B3LYP/6-311++G(d,p) method. (c) Simulated stick spectrum of *iso*-C_9H_7N according to anharmonic vibrational wavenumbers and IR intensities predicted with the B3LYP/6-311++G(d,p) method; only fundamental transitions are presented. The observed and predicted wavenumbers and IR intensities are listed in Table S9, ESI†.

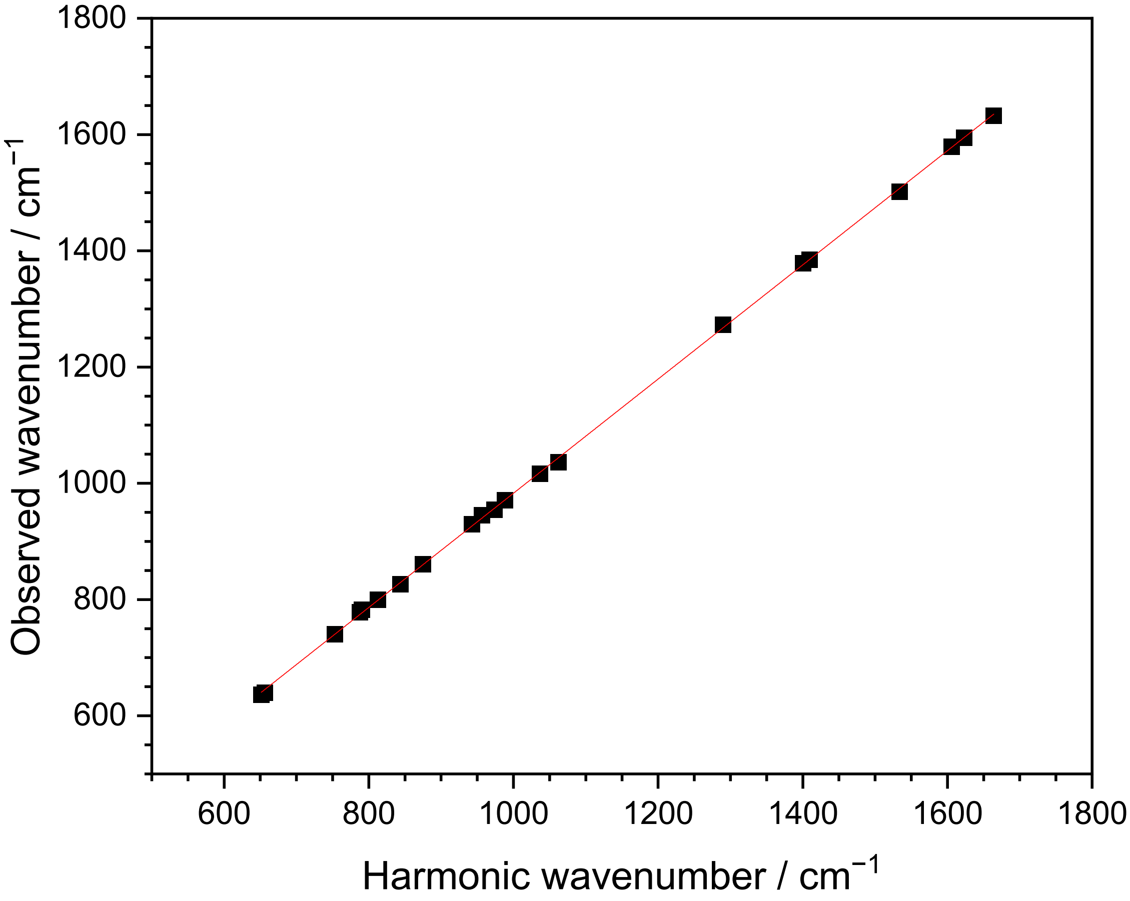

Fig. S8 Calibration curve for observed and calculated harmonic vibrational wavenumbers of *iso*-C_9H_7N in the region below 2000 cm^{-1}. From a linear regression analysis, we derived a scaling equation $y = (0.9823 \pm 0.0025)\, x + (0.6 \pm 2.8)$ for wavenumbers below 2000 cm^{-1}, in which y is the scaled vibrational wavenumber and x is the calculated harmonic vibrational wavenumber. The coefficient of determination (R^2) is 0.9999.

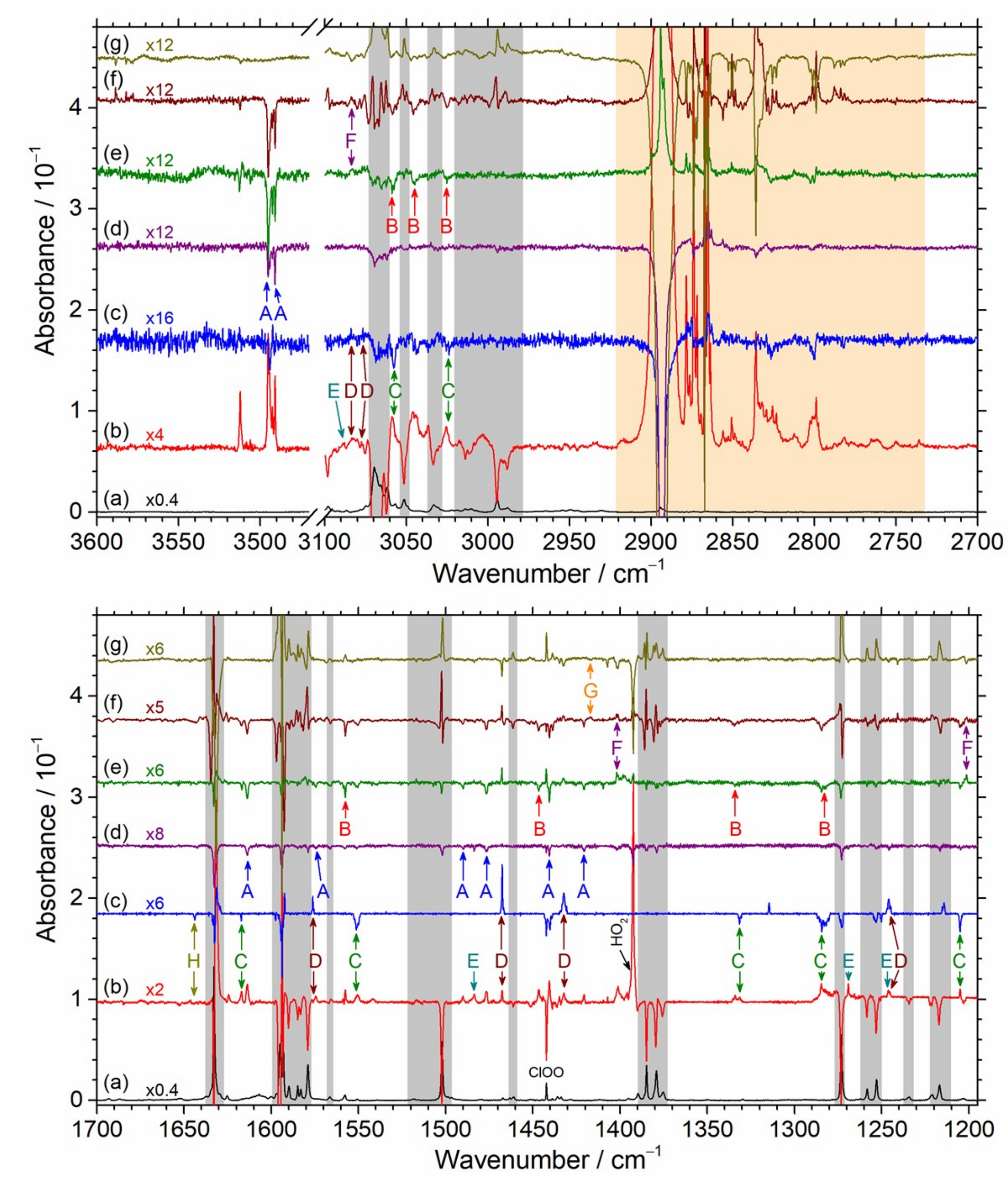

Fig. S9 Spectra of an *iso*-$C_9H_7N/Cl_2/p$-H_2 matrix in regions 3600−3470, 3100−2700, and 1700−1200 cm^{-1} at various stages of experiments. (a) Spectrum of an *iso*-$C_9H_7N/Cl_2/p$-H_2 matrix deposited at 3.2 K for 8 h and irradiated at 365 nm for 1 h. (b) Difference spectrum of the matrix after subsequent irradiation with IR light for 2 h. (c) Difference spectra of the matrix after further irradiation at 553 nm for 30 min. (d) Difference spectra of the sample after further irradiation at 540 nm for 30 min. (e) Difference spectra of the sample after further irradiation at 420 nm for 30 min. (f) Difference spectra of the sample after further irradiation at 405 nm for 30 min. (g) Difference spectra of the sample after further irradiation at 360 nm for 30 min. Lines in groups A (*iso*-C_9H_7NH), B (6-*iso*-HC_9H_7N), C (7-*iso*-HC_9H_7N), D (8-*iso*-HC_9H_7N), E (4-*iso*-HC_9H_7N), F (5-*iso*-HC_9H_7N), G (1-*iso*-HC_9H_7N), and H (3-*iso*-HC_9H_7N), are indicated. Spectral regions that suffer severe interference from absorption of *iso*-C_9H_7N are shaded gray and those from absorption of HCl and HCl complexes are shaded orange.

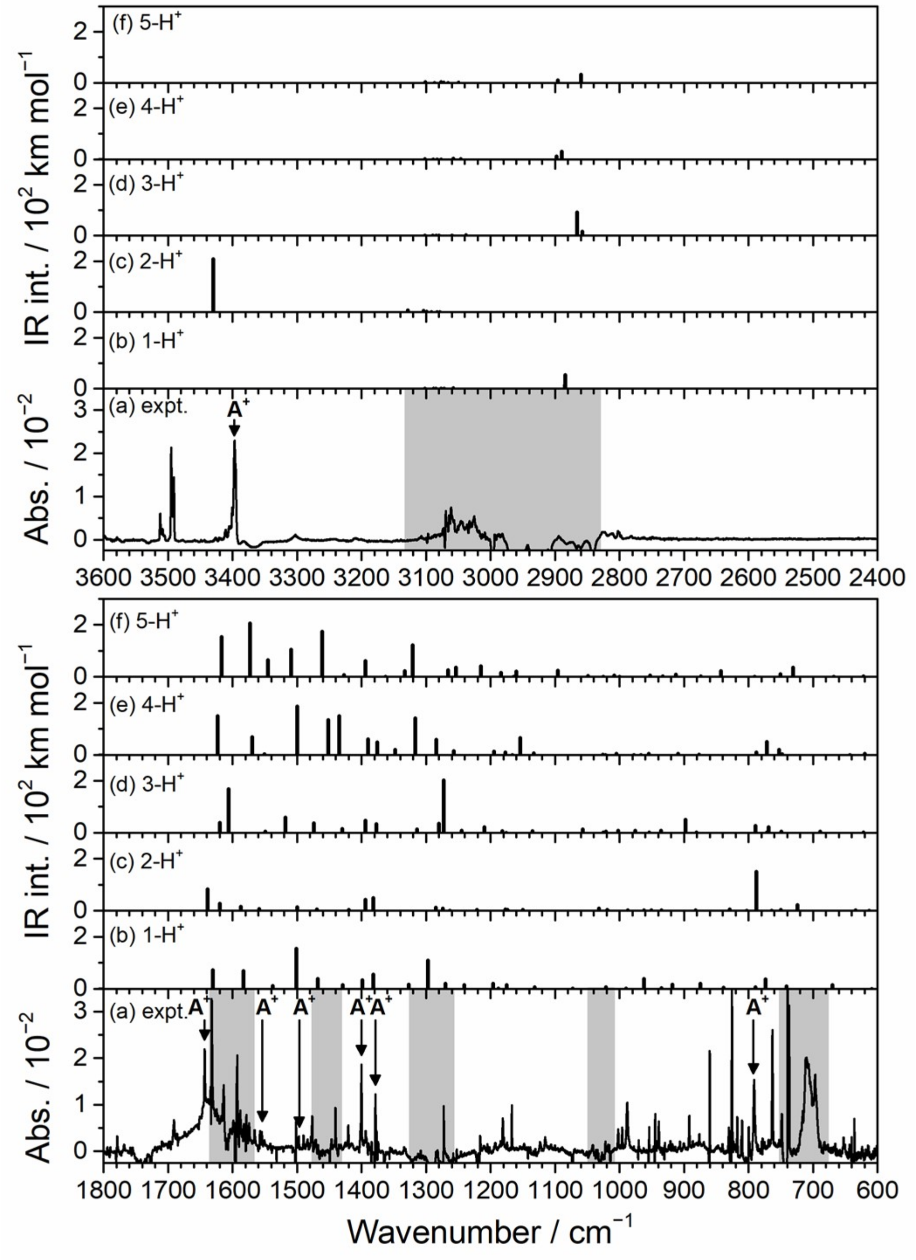

Fig. S10 Comparison of observed lines in group A$^+$ with predicted IR stick spectra of *iso*-$C_9H_8N^+$ isomers in regions 3600−2400 and 1800−600 cm^{-1}. (a) Spectrum of the electron-bombarded *iso*-C_9H_7N/*p*-H_2 matrix after stripping of lines of *iso*-C_9H_7N. Predicted IR spectra of 1-*iso*-$H^+C_9H_7N$ (b), *iso*-$C_9H_7NH^+$ (c), 2-$C_9H_7NH^+$), 3-*iso*-$H^+C_9H_7N$ (d), 4-*iso*-$H^+C_9H_7N$ (e), and 5-*iso*-$H^+C_9H_7N$ (f) simulated according to scaled harmonic wavenumbers and IR intensities predicted with the B3LYP/6-311++G(d,p) method. Lines in group A$^+$ are marked with arrows and spectral regions that suffer severe interference from absorption of C_9H_7N are shaded gray.

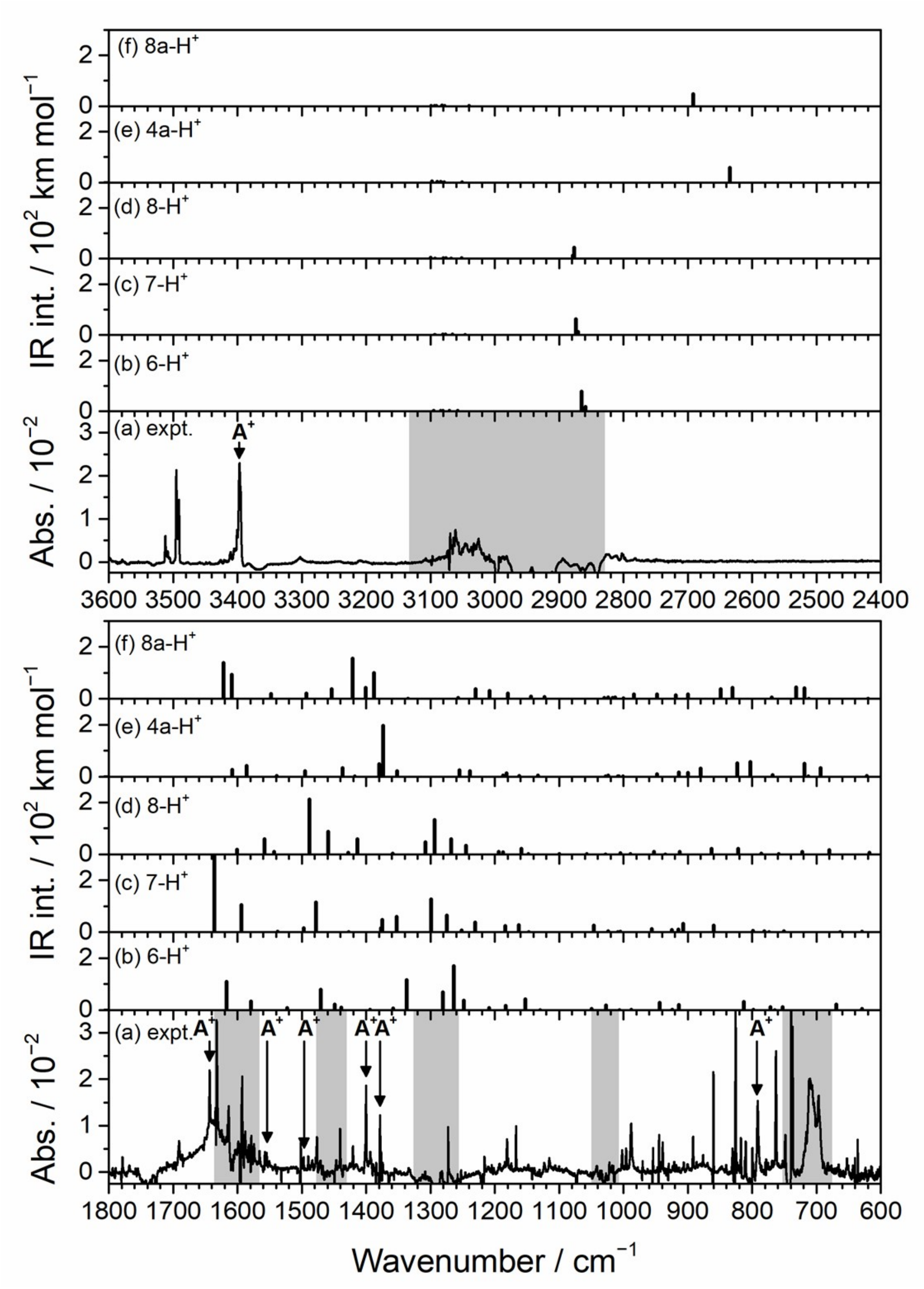

Fig. S11 Comparison of observed lines in group A^+ with the predicted IR stick spectra of *iso*-$C_9H_8N^+$ isomers in regions 3600−2400 and 1800−600 cm^{-1}. (a) Spectrum of the electron-bombarded *iso*-C_9H_7N/*p*-H_2 matrix after stripping of lines of *iso*-C_9H_7N. Predicted IR spectra of 6-*iso*-$H^+C_9H_7N$ (b), 7-*iso*-$H^+C_9H_7N$ (c), 8-*iso*-$H^+C_9H_7N$ (d), 4a-*iso*-$H^+C_9H_7N$ (e), and 8a-*iso*-$H^+C_9H_7N$ (f) simulated according to scaled harmonic wavenumbers and IR intensities predicted with the B3LYP/6-311++G(d,p) method. Lines in group A^+ are marked with arrows and spectral regions that suffer severe interference from absorption of *iso*-C_9H_7N are shaded gray.

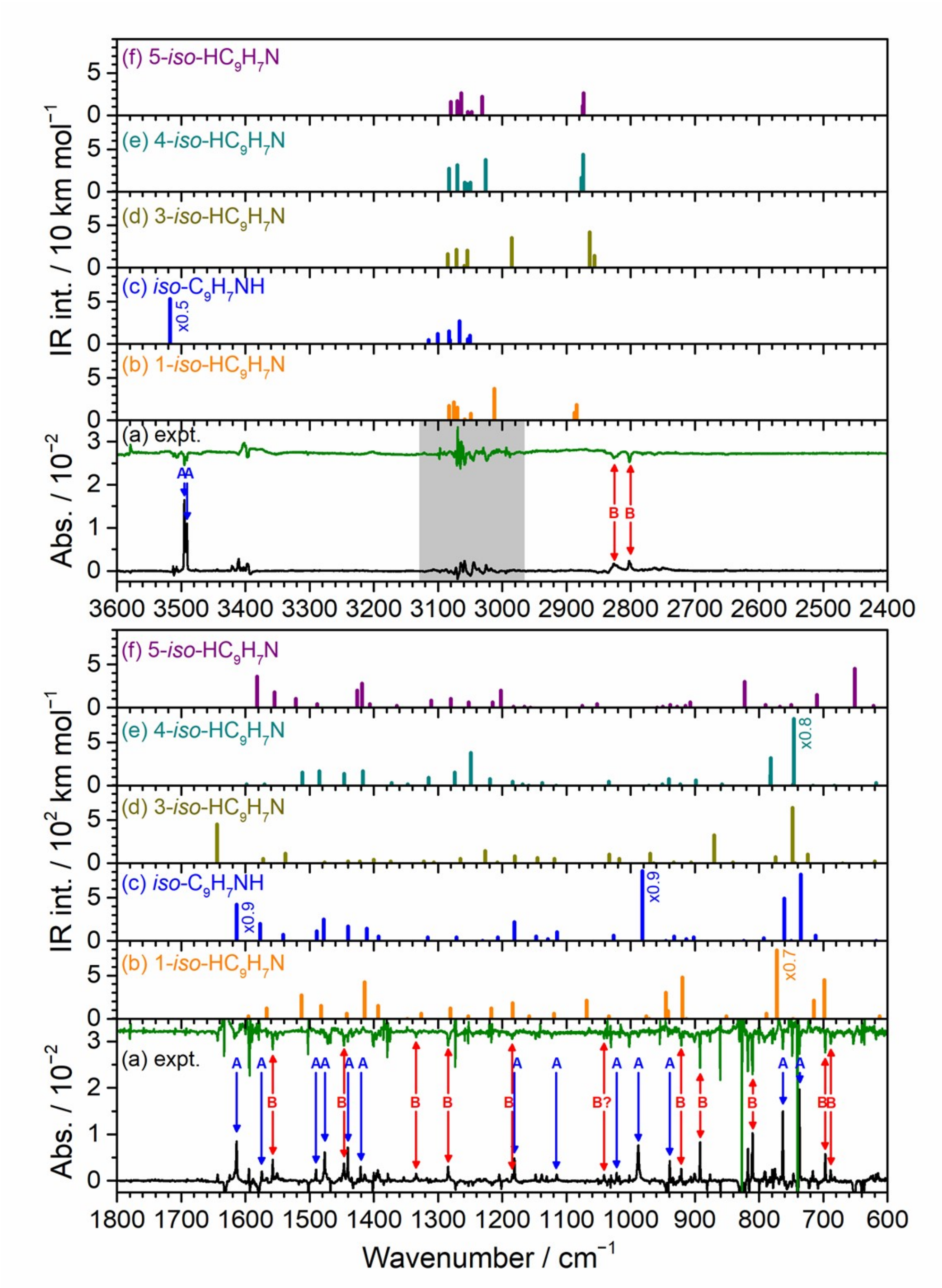

Fig. S12 Comparison of observed lines of groups A and B in regions 3600−2400 and 1800−600 cm^{-1} in electron bombardment experiments on *iso*-C_9H_7N with IR stick spectra of 1- to 5-*iso*-C_9H_8N predicted with theory. (a) Difference spectra after secondary irradiation at 365 nm (lower trace, inverted) and after secondary irradiation at 405 nm (upper trace) of the electron-bombarded *iso*-C_9H_7N/*p*-H_2 matrix; lines of groups A and B are indicated with blue and red arrows, respectively. Predicted IR spectra of 1-*iso*-HC_9H_7N (b), C_9H_7NH (c, 2-*iso*-C_9H_7NH), 3-*iso*-HC_9H_7N (d), 4-*iso*-HC_9H_7N (e), and 5-*iso*-HC_9H_7N (f) simulated according to scaled harmonic wavenumbers and IR intensities predicted with the B3LYP/6-311++G(d,p) method. Spectral regions that suffer severe interference from absorption of C_9H_7N are shaded gray.

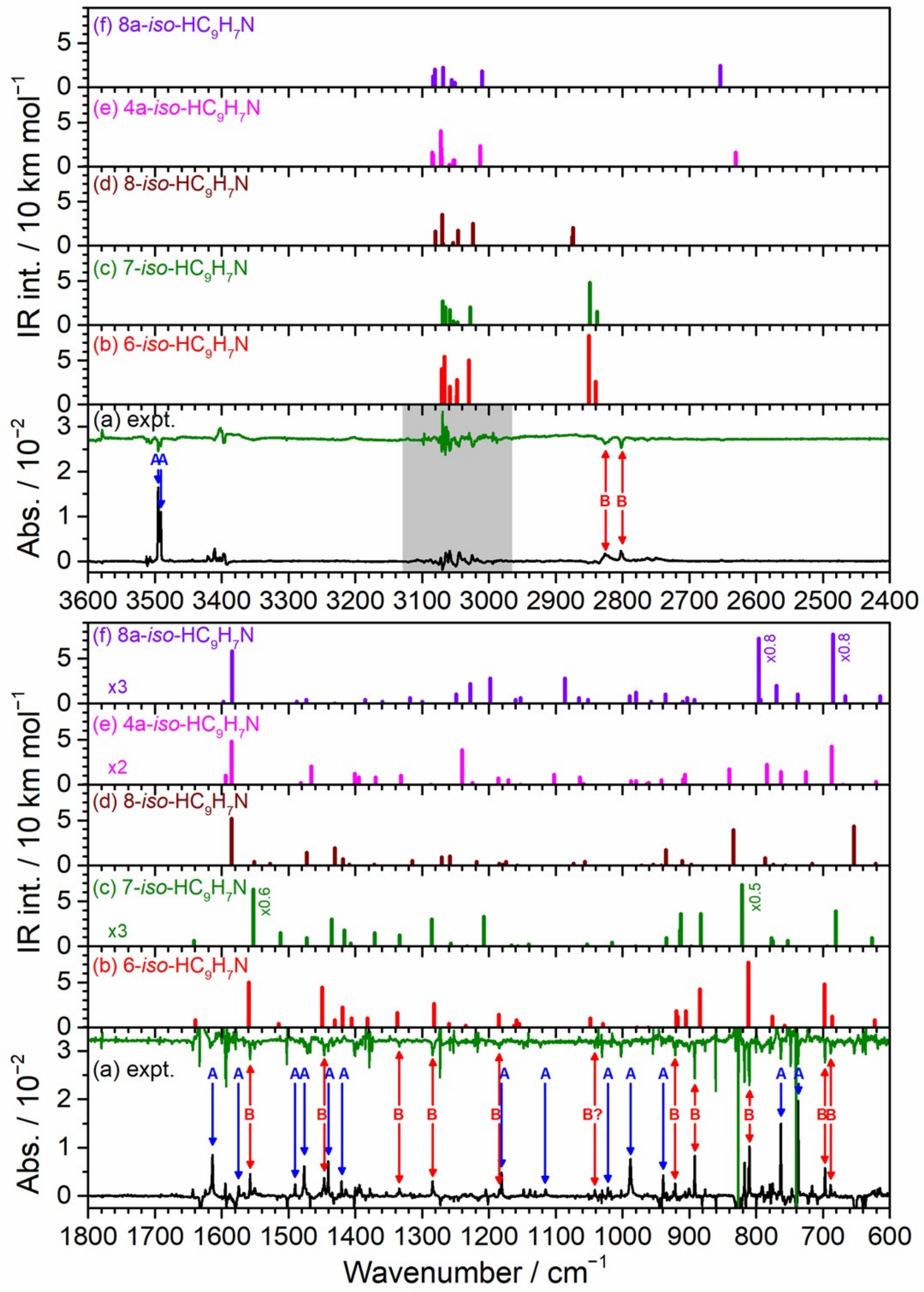

Fig. S13 Comparison of observed lines of groups A and B in regions 3600−2400 and 1800−600 cm^{-1} in electron bombardment experiments on *iso*-C_9H_7N with IR stick spectra of 6-, 7-, 8-, 4a-, and 8a-*iso*-C_9H_8N predicted with theory. (a) Difference spectra after secondary irradiation at 365 nm (lower trace, inverted) and after secondary irradiation at 405 nm (upper trace) of the electron-bombarded *iso*-C_9H_7N/*p*-H_2 matrix; lines of groups A and B are indicated with blue and red arrows, respectively. Predicted IR spectra of 6-*iso*-HC_9H_7N (b), 7-*iso*-HC_9H_7N (c), 8-*iso*-HC_9H_7N (d), 4a-*iso*-HC_9H_7N (e), and 8a-*iso*-HC_9H_7N (f) simulated according to scaled harmonic wavenumbers and IR intensities predicted with the B3LYP/6-311++G(d,p) method. Spectral regions that suffer severe interference from absorption of C_9H_7N are shaded gray.

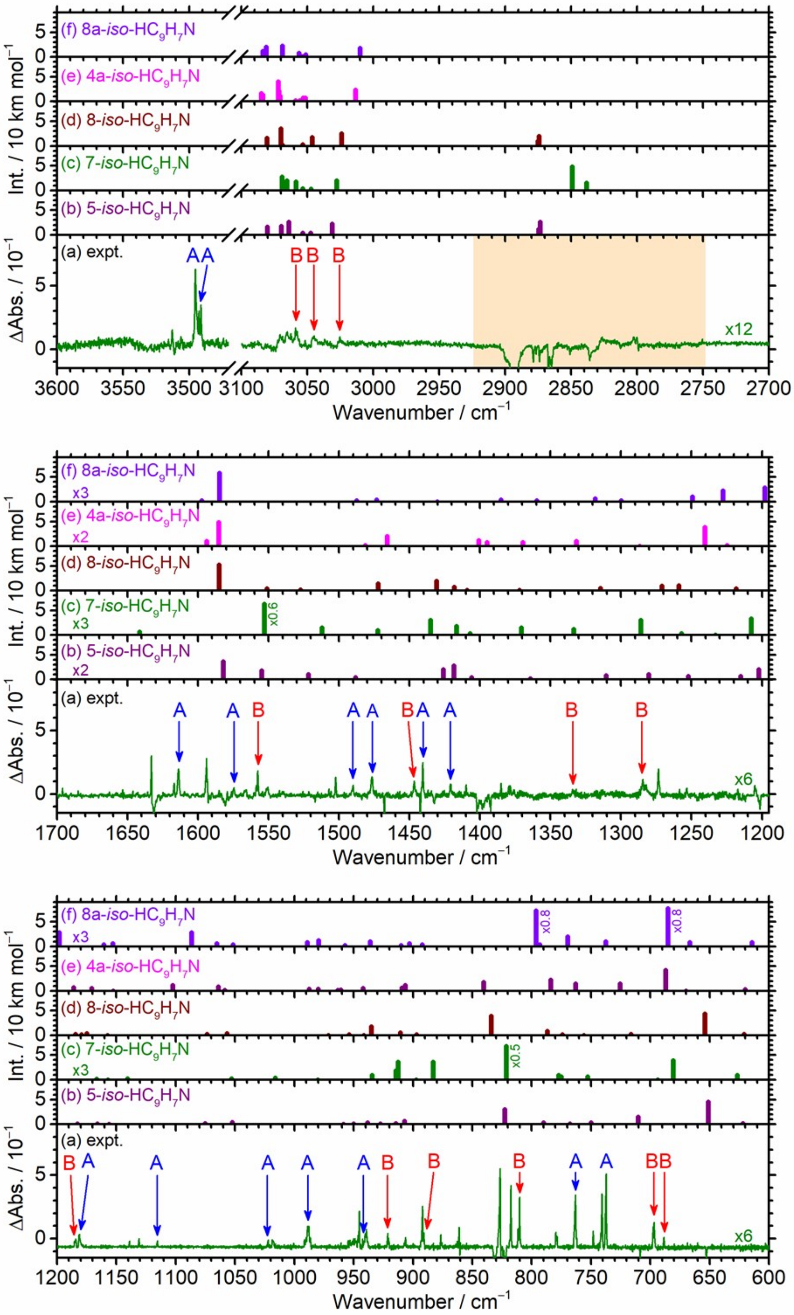

Fig. S14 Comparison of observed lines of group A and group B in regions 3600−3450 and 3100−2700 and 1700−600 cm^{-1} in *iso*-$C_9H_7N/Cl_2/p$-H_2 experiments with IR stick spectra of *iso*-C_9H_8N predicted with theory. (a) Difference spectrum after 420 nm irradiation, inverted Fig. 3e; lines belonging to group A (*iso*-C_9H_7NH) and group B (6-*iso*-HC_9H_7N) are indicated with blue and red arrows, respectively. IR stick spectra of 5-*iso*-HC_9H_7N (b), 7-*iso*-HC_9H_7N (c), 8-*iso*-HC_9H_7N (d), 4a-*iso*-HC_9H_7N (e), and 8a-*iso*-HC_9H_7N (f) simulated according to scaled harmonic vibrational wavenumbers and harmonic IR intensities predicted with the B3LYP/6-311++G(d,p) method. Spectral regions that suffer severe interference from absorption of HCl and HCl complexes are shaded orange.

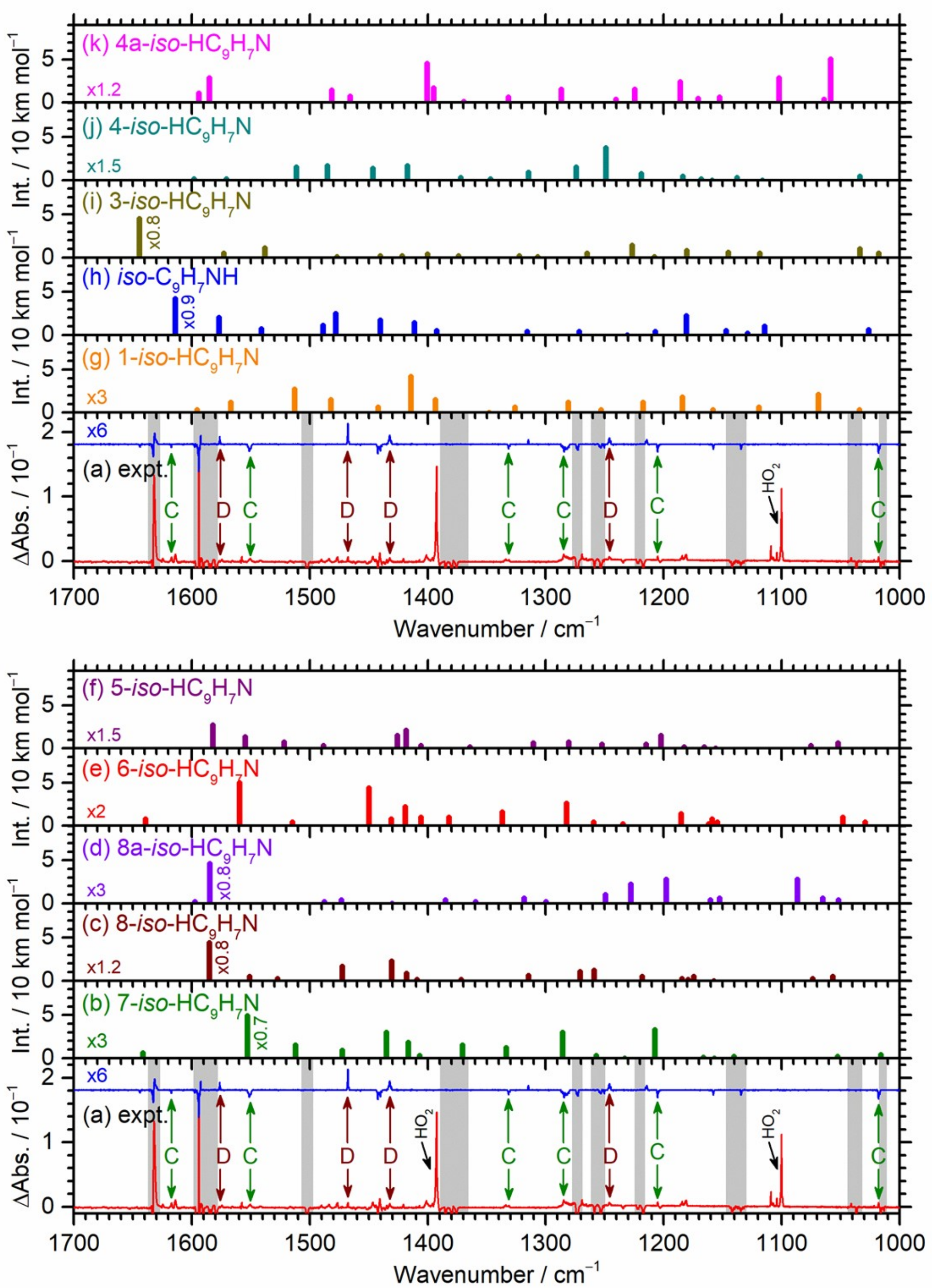

Fig. S15 Comparison of observed lines of groups C and D in region 1700−1000 cm^{-1} in *iso*-$C_9H_7N/Cl_2/p$-H_2 experiments with IR stick spectra of *iso*-C_9H_8N predicted with theory. (a) Difference spectrum after IR irradiation (lower trace), Fig. 3b, and after secondary irradiation at 553 nm (upper trace), Fig. 3c; lines belonging to group C (7-*iso*-C_9H_7NH) and group D (8-*iso*-HC_9H_7N) are indicated with green and brown arrows, respectively. IR stick spectra of 7-*iso*-HC_9H_7N (b), 8-*iso*-HC_9H_7N (c), 8a-*iso*-HC_9H_7N (d), 6-*iso*-HC_9H_7N (e), 5-*iso*-HC_9H_7N (f), 1-*iso*-HC_9H_7N (g), *iso*-C_9H_7NH (h), 3-*iso*-HC_9H_7N (i), 4-*iso*-HC_9H_7N (j), and 4a-*iso*-HC_9H_7N (k) simulated according to scaled harmonic vibrational wavenumbers and harmonic IR intensities predicted with the B3LYP/6-311++G(d,p) method. Spectral regions that suffer severe interference from absorption of C_9H_7N are shaded gray.

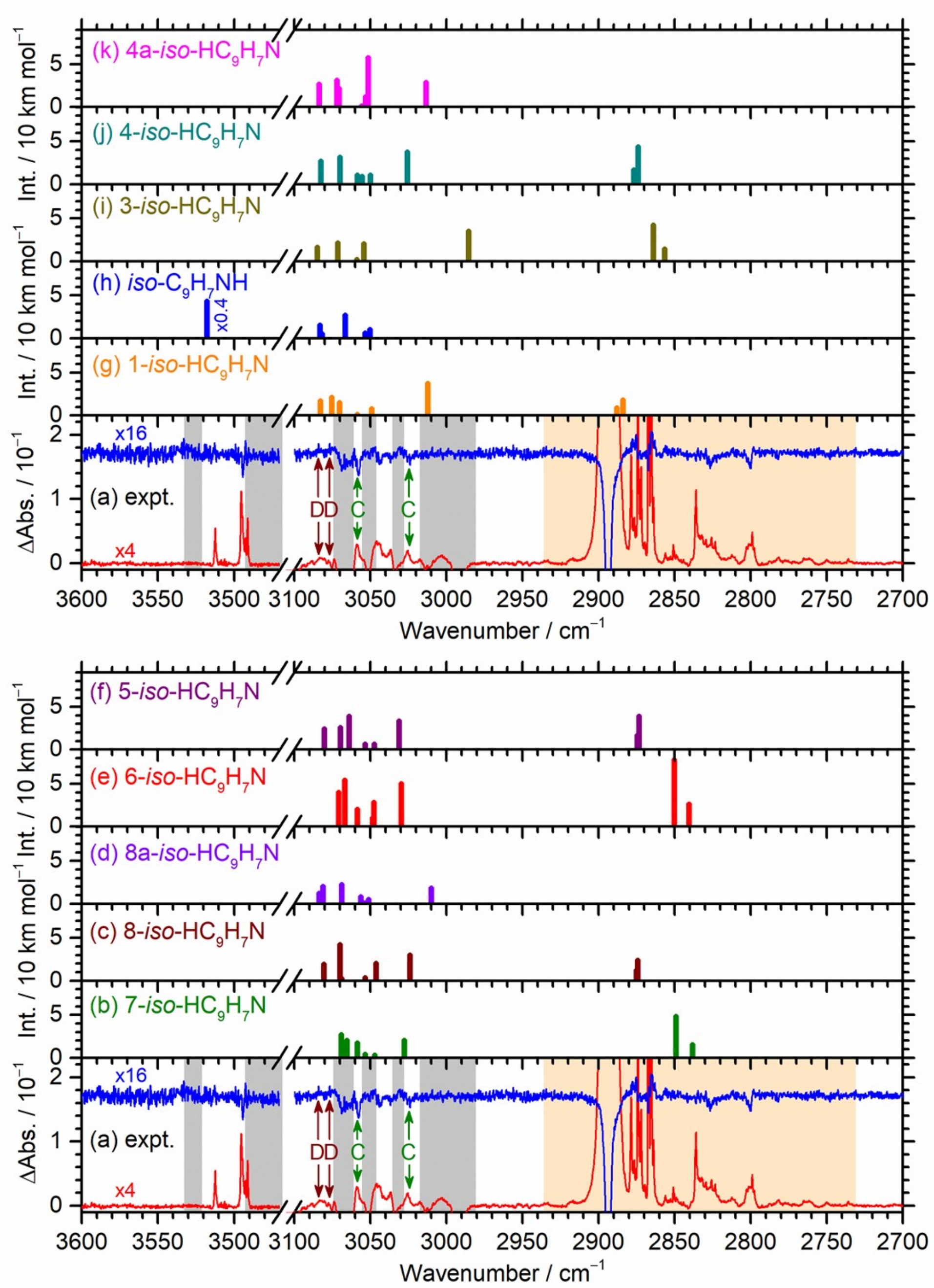

Fig. S16 Comparison of observed lines of groups C and D in regions 3600−3450 and 3100−2700 cm^{-1} in *iso*-$C_9H_7N/Cl_2/p$-H_2 experiments with IR stick spectra of *iso*-C_9H_8N predicted with theory. (a) Difference spectrum after IR irradiation (lower trace), Fig. 3b, and after secondary irradiation at 553 nm (upper trace), Fig. 3c; lines belonging to group C (7-*iso*-C_9H_7NH) and group D (8-*iso*-HC_9H_7N) are indicated with green and brown arrows, respectively. IR stick spectra of 7-*iso*-HC_9H_7N (b), 8-*iso*-HC_9H_7N (c), 8a-*iso*-HC_9H_7N (d), 6-*iso*-HC_9H_7N (e), 5-*iso*-HC_9H_7N (f), 1-*iso*-HC_9H_7N (g), *iso*-C_9H_7NH (h), 3-*iso*-HC_9H_7N (i), 4-*iso*-HC_9H_7N (j), and 4a-*iso*-HC_9H_7N (k) simulated according to scaled harmonic vibrational wavenumbers and harmonic IR intensities predicted with the B3LYP/6-311++G(d,p) method.

Spectral regions that suffer severe interference from absorption of C_9H_7N are shaded gray.

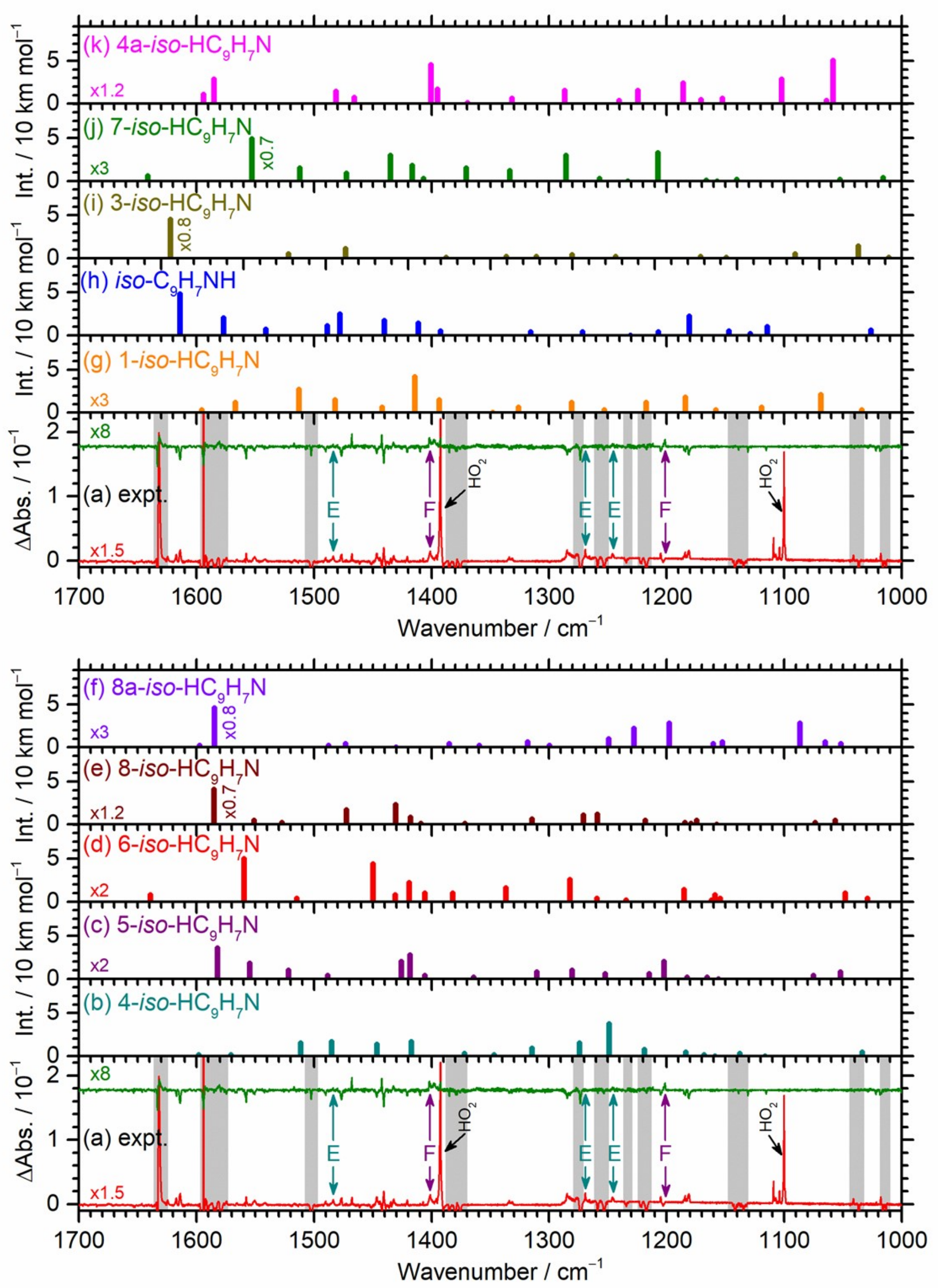

Fig. S17 Comparison of observed lines of groups E and F n region 1700−1000 cm^{-1} in *iso*-C$_9$H$_7$N/Cl$_2$/*p*-H$_2$ experiments with IR stick spectra of *iso*-C$_9$H$_8$N predicted with theory. (a) Difference spectrum after IR irradiation (lower trace), Fig. 3b, and after secondary irradiation at 420 nm (upper trace), Fig. 3e; lines belonging to group E (4-*iso*-C$_9$H$_7$NH) and group F (5-*iso*-HC$_9$H$_7$N) are indicated with light blue and purple arrows, respectively. IR stick spectra of 4-*iso*-HC$_9$H$_7$N (b), 5-*iso*-HC$_9$H$_7$N (c), 6-*iso*-HC$_9$H$_7$N (d), 8-*iso*-HC$_9$H$_7$N (e), 8a-*iso*-HC$_9$H$_7$N (f), 1-*iso*-HC$_9$H$_7$N (g), *iso*-C$_9$H$_7$NH (h), 3-*iso*-HC$_9$H$_7$N (i), 7-*iso*-HC$_9$H$_7$N (j), and 4a-*iso*-HC$_9$H$_7$N (k) simulated according to scaled harmonic vibrational wavenumbers and harmonic IR intensities predicted with the B3LYP/6-311++G(d,p) method. Spectral regions that suffer severe interference from absorption of C_9H_7N are shaded gray.

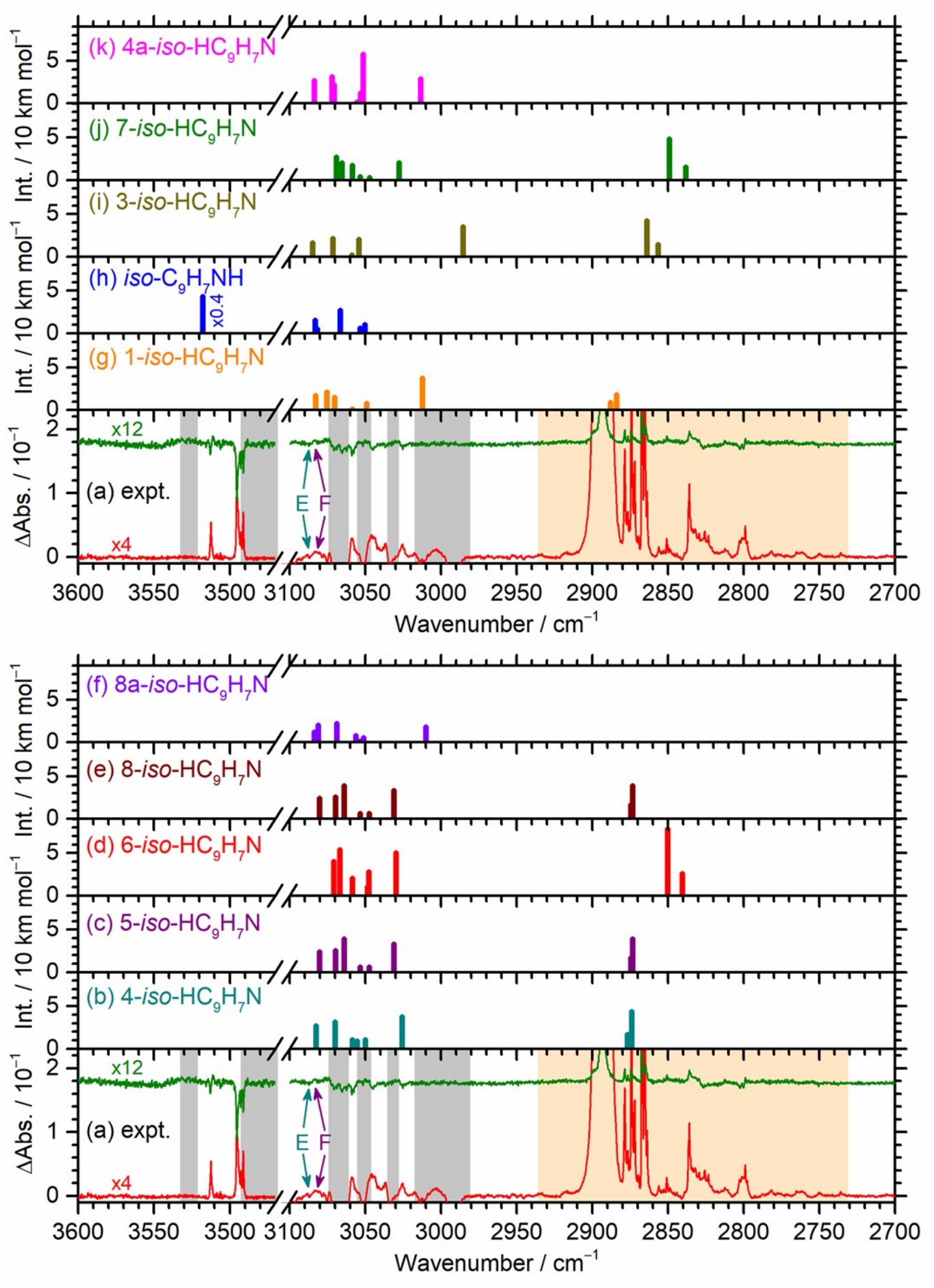

Fig. S18 Comparison of observed lines of groups E and F in regions 3600−3450 and 3100−2700 cm^{-1} in *iso*-$C_9H_7N/Cl_2/p$-H_2 experiments with IR stick spectra of *iso*-C_9H_8N predicted with theory. (a) Difference spectrum after IR irradiation (lower trace), Fig. 3b, and after secondary irradiation at 420 nm (upper trace), Fig. 3e; lines belonging to group E (4-*iso*-C_9H_7NH) and group F (5-*iso*-HC_9H_7N) are indicated with light blue and purple arrows, respectively. IR stick spectra of 4-*iso*-HC_9H_7N (b), 5-*iso*-HC_9H_7N (c), 6-*iso*-HC_9H_7N (d), 8-*iso*-HC_9H_7N (e), 8a-*iso*-HC_9H_7N (f), 1-*iso*-HC_9H_7N (g), *iso*-C_9H_7NH (h), 3-*iso*-HC_9H_7N (i), 7-*iso*-HC_9H_7N (j), and 4a-*iso*-HC_9H_7N (k) simulated according to scaled harmonic vibrational wavenumbers and harmonic IR intensities predicted with the B3LYP/6-311++G(d,p) method. Spectral regions that suffer severe interference from absorption of C_9H_7N are shaded gray and those from absorption of HCl and HCl complexes are shaded orange.

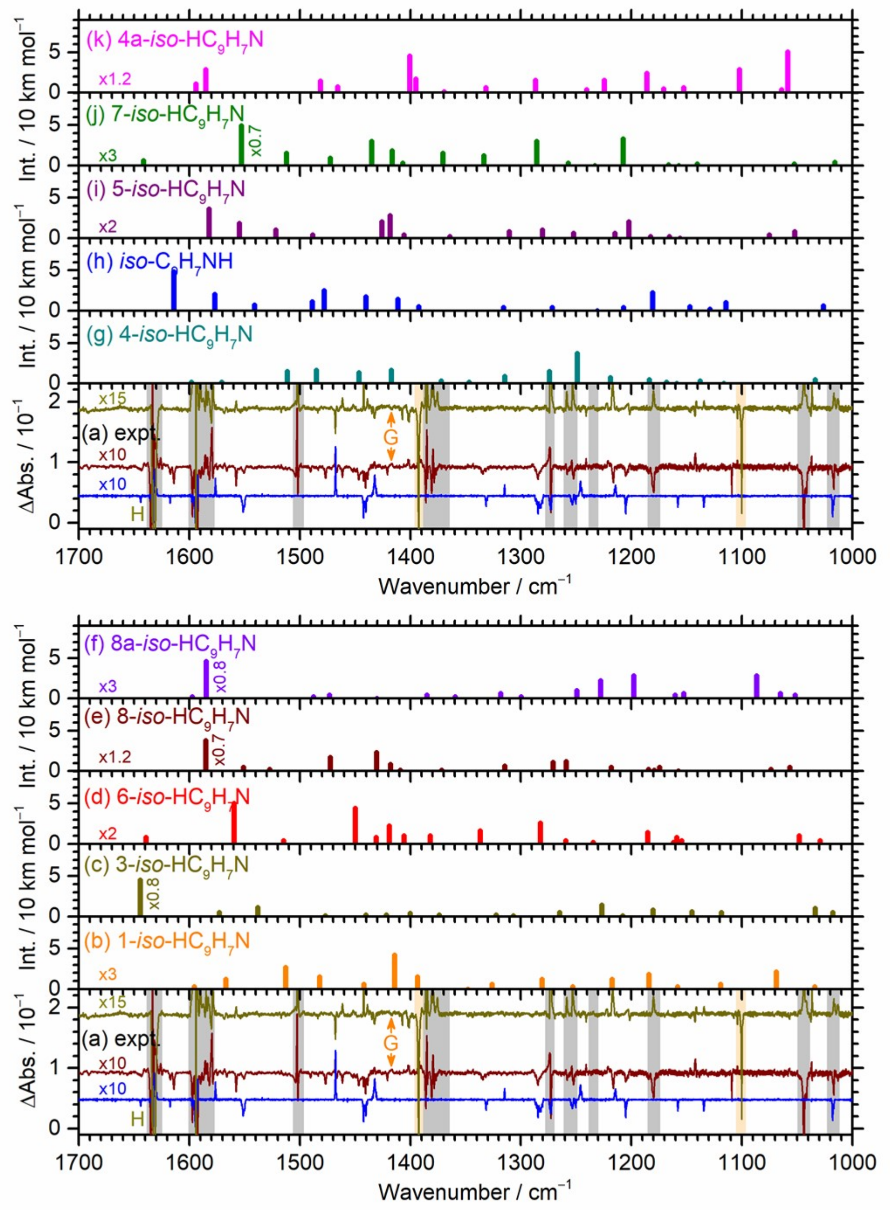

Fig. S19 Comparison of observed lines of groups G and H in region 1700−1000 cm^{-1} in iso-$C_9H_7N/Cl_2/p\text{-}H_2$ experiments with IR stick spectra of iso-C_9H_8N predicted with theory. (a) Difference spectrum after secondary irradiation at 553 nm (lower trace), Fig. 3c, after secondary irradiation at 405 nm (middle trace), Fig. 3f, and after secondary irradiation at 360 nm (upper trace), Fig. 3g; lines belonging to group G (1-iso-C_9H_7NH) and group H (3-iso-HC_9H_7N) are indicated with orange and olive arrows, respectively. IR stick spectra of 1-iso-HC_9H_7N (b), 3-iso-HC_9H_7N (c), 6-iso-HC_9H_7N (d), 8-iso-HC_9H_7N (e), 8a-iso-HC_9H_7N (f), 4-iso-HC_9H_7N (g), iso-C_9H_7NH (h), 5-iso-HC_9H_7N (i), 7-iso-HC_9H_7N (j), and 4a-iso-HC_9H_7N (k) simulated according to scaled harmonic vibrational wavenumbers and harmonic IR intensities predicted with the B3LYP/6-311++G(d,p) method. Spectral regions that suffer severe interference from absorption of C_9H_7N are shaded gray.

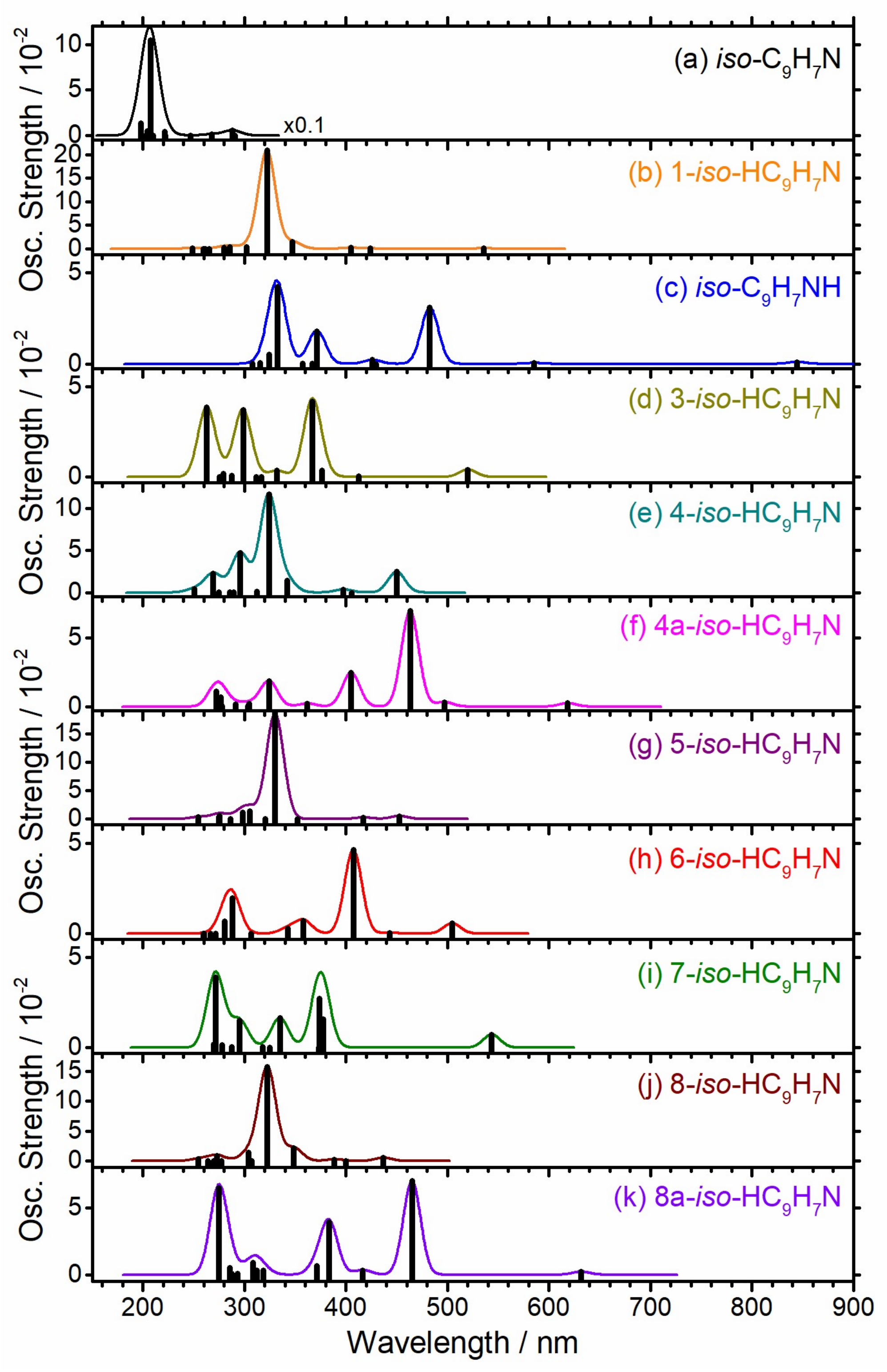

Fig. S20 UV spectra of *iso*-C_9H_7N and various isomers of *iso*-C_9H_8N simulated with the TD-B3LYP/6-311++G(d,p) method. (a) *iso*-C_9H_7N, (b) 1-*iso*-HC_9H_7N, (c) *iso*-C_9H_7NH, (d) 3-*iso*-HC_9H_7N, (e) 4-*iso*-HC_9H_7N, (f) 4a-*iso*-HC_9H_7N, (g) 5-*iso*-HC_9H_7N, (h) 6-*iso*-HC_9H_7N, (i) 7-*iso*-HC_9H_7N, (j) 8-*iso*-HC_9H_7N, and (k) 8a-*iso*-HC_9H_7N The spectra were convoluted with a full width 30 nm at half maximum.

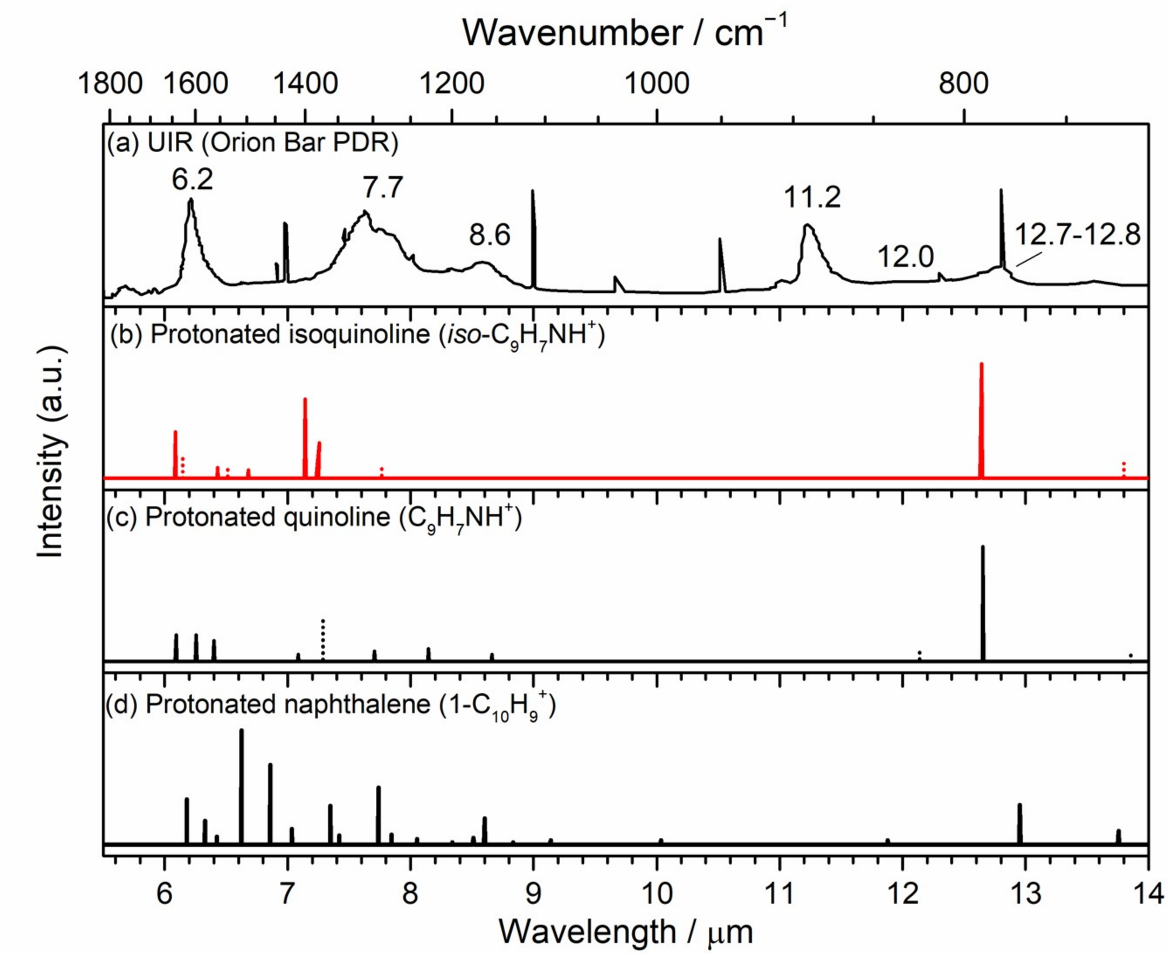

Fig. S21 Comparison of UIR bands with observed stick IR spectra of protonated isoquinoline, protonated quinoline, and protonated naphthalene. (a) The UIR emission spectrum from Orion Bar PDR. (E. Peeters, L. J. Allamandola, D. M. Hudgins, S. Hony and A. G. G. M. Tielens, *Astrophysics of Dust*, eds. A. N. Witt, G. C. Clayton and B. T. Draine, 2004, **309**, 141) Experimental spectra of (b) protonated isoquinoline (*iso*-$C_9H_7NH^+$, this work), (c) protonated quinoline ($C_9H_7NH^+$, C.-Y. Tseng, Y.-J. Wu and Y.-P. Lee, *J. Phys. Chem. A*, 2022, **126**, 2361–2372), and (d) protonated naphthalene (1-$C_{10}H_9^+$, M. Bahou, Y.-J. Wu and Y.-P. Lee, *Phys. Chem. Chem. Phys.* 2013, **15**, 1907–1917) are presented with sticks of which the heights represent integrated intensities. Major quantum-chemically predicted but unobserved lines are presented in dashed lines.